Discussion Paper

Time-varying state correlations in state space models and their estimation via indirect inference

Caterina Schiavoni

Siem Jan Koopman
Franz Palm
Stephan Smeekes
Jan van den Brakel

February, 2021

Statistics Netherlands uses a state space model to estimate the Dutch unemployment by using monthly series about the labour force surveys (LFS). More accurate estimates of this variable can be obtained by including auxiliary information in the model, such as the univariate administrative series of claimant counts. Legislative changes and economic crises may affect the relation between survey-based and auxiliary series. This time-changing relationship is captured by a time-varying correlation parameter in the covariance matrix of the transition equation's error terms. We treat the latter parameter as a state variable, which makes the state space model become nonlinear and therefore its estimation by Kalman filtering and maximum likelihood infeasible. We therefore propose an indirect inference approach to estimate the static parameters of the model, which employs cubic splines for the auxiliary model, and a bootstrap filter method to estimate the time-varying correlation together with the other state variables of the model. We conduct a Monte Carlo simulation study that shows that our proposed methodology is able to correctly estimate both the time-constant parameters and the state vector of the model. Empirically we find that the financial crisis of 2008 triggered a deeper and more prolonged deviation between the survey-based and the claimant counts series, than a legislative change in 2015. Promptly tackling such changes, which our proposed method does, results in more realistic real-time unemployment estimates.

bootstrap filter, cubic splines, indirect inference, nonlinear state space, time-varying parameter, unemployment

This work was funded by the European Union under grant no. 07131.2017.003-2017.596. The views expressed in this paper are those of the authors and do not necessarily reflect the policy of Statistics Netherlands. Previous versions of this paper have been presented at the OECD Workshop on Time Series Methods for Official Statistics 2019, the NPSO Innovatiedag 2019, the 12th World Congress of the Econometric Society 2020, BigSurv2020, and internal seminars organised by Maastricht University and Statistics Netherlands. We thank conference and seminar participants for their useful feedbacks.

1 Introduction

Official statistics about the labour force, as published by national statistical institutes, are generally based on survey data collected via a rotating panel design in combination with direct estimation procedures, such as the general regression (GREG) estimator (Särndal et al., 1992). Direct or design-based estimators have nice statistical properties under large sample sizes, but the variance of these estimates rapidly become unacceptably large in case of small sample sizes (Rao and Molina, 2015). Small sample sizes typically occur if estimates for short reference periods or estimates at a detailed regional level are required. As a result most national statistical institutes publish quarterly or rolling quarterly figures about the labour force. Since monthly figures are more timely and relevant for policy makers and GREG estimates for monthly labour force figures are not precise enough, Statistic Netherlands implemented a state space model for the production of official monthly labour force figures. This model is used as a form of small area estimation (Rao and Molina, 2015), by using the labour force survey (LFS) data collected over many months to improve the estimates for the current month. The model also accounts for rotation group bias (Bailar, 1975), and serial correlation in the survey errors due to the rotating panel design of the Dutch LFS (Pfeffermann, 1991; van den Brakel and Krieg, 2015).

The aforementioned state space model estimates the Dutch unemployed[1)] as an unobserved trend and seasonal component. The state space structure allows to model not only the unemployment itself, but also its change, its seasonality, the survey errors, and the rotation group bias that affects the observed series from the labour force survey. The estimation accuracy of the unemployment can be further improved by augmenting the model with auxiliary series that might be related to it. Harvey and Chung (2000), van den Brakel and Krieg (2016) and Schiavoni et al. (2021) show that the monthly univariate auxiliary series of claimant counts, which is a registry source, can significantly improve the estimation accuracy of the unemployment.

In this paper we augment the Dutch labour force state space model with the auxiliary series of claimant counts, and we model the relationship between survey-based and auxiliary series as time-varying. This is the main novelty of the paper. Modeling relationships between variables as time-varying allows to tackle changes that are triggered, for instance, by economic crises. Time-changing relations between different sources of data that aim at measuring the same variables, can also be due to legislative changes.

We let the time-varying relation be captured by a time-varying correlation in the covariance matrix of the disturbances of the state space model's transition equation. Solving our problem, i.e., extracting this time-varying state correlation, is therefore already challenged by the fact that this parameter relates innovations of components that are unobserved. Additionally, data and respective log-likelihood functions, are much less informative about correlations than other parameters, such as means or variances.

[1)] Throughout the paper, we use the terms "unemployment", "unemployed" and "unemployed labour force" interchangeably to indicate the total number of unemployed people.

We treat the time-varying correlation that enters this covariance matrix as an additional state variable with its own dynamic equation, which makes this parameter random, i.e. subject to its own source of error. The state space model therefore becomes nonlinear. The nonlinearity of the model hampers the estimation of the state variables by standard Kalman filtering, which in turns makes the likelihood function (needed to estimate the static parameters of the model) intractable. There are several frequentist methods that can be employed in order to estimate nonlinear state space models. Importance sampling (see Jungbacker and Koopman (2007), Koopman et al. (2015), and Koopman et al. (2018)) and the Extended Kalman filter (explained in Durbin and Koopman (2012, Chapter 10)) are some examples, and they allow to estimate both the state variables and the time-constant parameters of the nonlinear model. The reprojection method of Gallant and Tauchen (1998) is another technique that can be employed in order to estimate the state vector but not the static parameters of nonlinear state space models. Nonetheless, the implementation of these methods in our setting is hampered by the nonlinearity being in the transition equation and involving not only state variables but also disturbance terms (as will become clear at the beginning of Section 3). The above-mentioned methods are more suited to solve nonlinearities appearing in the observation equation or involving only state variables. Shifting our nonlinear problem from the transition to the observation equation is non-trivial. Alternatively, sequential Monte Carlo methods, such as particle filtering, can be employed (and we do) for the estimation of the state vector, but the resulting log-likelihood function is not continuous with respect to the static parameters of the nonlinear model, which hinders their estimation via this approach (Creal, 2012). We circumvent this problem by estimating the time-constant parameters by indirect inference, before applying particle filtering.

The indirect inference method, originally proposed by Gourieroux et al. (1993), requires the use of an auxiliary model which approximates the true one, but which can also be easily estimated. In our case the auxiliary model employs a deterministic specification for the time-varying correlation, which preserves the linearity of the state space model. This deterministic specification assumes a smooth change over time for the correlation, and is based on the cubic splines estimation method. The latter approach requires the change points in time to be chosen a priori, and can already be employed, by itself, in estimating the time-varying state correlation. Koopman et al. (2006) and Proietti and Hillebrand (2017) already utilised this method for modeling time-varying parameters in state space models. However, the use of cubic splines for the auxiliary model in the indirect inference estimation of static parameters, not only in state space models, has not been explored before. Once the time-constant parameters have been estimated by indirect inference, we employ a Rao-Blackwellised (Chen and Liu, 2000) bootstrap filter (Gordon et al., 1993), which is a type of sequential Monte Carlo algorithm, and more specifically of particle filter, in order to estimate the state variables of the model. The Rao-Blackwellisation of the bootstrap filter is needed in order to simplify the estimation of the state vector when this is large, which is the case in the Dutch labour force model extended with the claimant counts series.

Monfardini (1998) and Gagliardini et al. (2017) are very close works to our paper as they both employ indirect inference in order to estimate the static parameters of nonlinear state space models, where the nonlinearity arises from stochastic variances in the innovations of the observation equation. In the former paper Autoregressive and Moving Average (ARMA) are employed as auxiliary models, whereas the latter work

makes use of Mixed Data Sampling (MIDAS) regressions and Autoregressive Conditional Heteroskedasticity (ARCH) models, and it also provides a filtering step for the estimation of state variables based on the reprojection method of Gallant and Tauchen (1998). Stochastic variances are a rather common source of nonlinearity in state space models and there are many, also applied, papers that deal with them. Stock and Watson (2007) and Antolin-Diaz et al. (2017) are two examples, and they consider nonlinear state space models, respectively for US inflation and a set of US macroeconomic variables, where both the innovations in the measurement and transition equations have stochastic variances. The models are estimated via the Bayesian approach of Markov Chain Monte Carlo (MCMC), which could probably also be employed to estimate our nonlinear model, but we do not venture into Bayesian techniques. Both papers show how recession periods can play a big role in triggering changes in parameters, in their cases by boosting volatilities. To the best of our knowledge, our paper is the first one to deal with the estimation of a stochastic state correlation, and that therefore employs particle filtering for this purpose.

We conduct a Monte Carlo simulation study in order to assess the performance of our proposed estimation methods: the one purely based on cubic splines, and the one which combines indirect inference and Rao-Blackwellised bootstrap filtering. We investigate not only how they are able to estimate the time-constant parameters of the model as well as the true time-varying relation, but also to which extent estimating this relation as time-varying, instead of time-constant, yields gains in the estimation accuracy of unobserved components of interest. We then conduct an empirical study to estimate the Dutch unemployment by means of the labour force state space model augmented with the auxiliary series of claimant counts, while modeling the relationship between survey-based and auxiliary series as time-varying, with our proposed methods.

The paper is structured as follows. Section 2 presents a description of the state space model used by Statistics Netherlands for estimating monthly unemployment figures, and its extension with the univariate auxiliary series of claimant counts. Section 3 describes our proposed methods for the estimation of the time-varying correlation, together with the remaining state variables and the static parameters of the nonlinear state space model. Sections 4 and 5 report the results of, respectively, the Monte Carlo simulation study and the empirical application. Finally, Section 6 concludes the paper.

2 The Dutch labour force model and its extension

The Dutch LFS is conducted according to a rotating panel design. Each month a new sample, drawn according to the stratified two-stage cluster design described in van den Brakel and Krieg (2015) and Schiavoni et al. (2021), enters the panel and is interviewed five times at quarterly intervals. After the fifth interview, the sample leaves the panel. The sample that is interviewed for the j^{th} time is called the j^{th} wave of the panel, for $j = 1, \ldots, 5$. This rotation design implies that in each month five samples are observed, which over time generate a five-dimensional time series of the survey-based

unemployed labour force, defined as population total (see Schiavoni et al. (2021) for a visualisation of the rotation panel design of the Dutch LFS).

Let $y_{j,t}$ denote the general regression (GREG) estimate (Särndal et al., 1992) for the Dutch unemployment in month t based on the sample observed in wave j. Now $y_t = \left(y_{1,t}, \ldots, y_{5,t}\right)'$ denotes the vector with the five GREG estimates for the Dutch unemployment in month t. This five-dimensional vector of GREG estimates is cast in a state space model whose measurement equation takes the expression:

$$y_t = 1_5 \theta_{y,t} + \lambda_t + e_t, \tag{2.1}$$

where 1_5 is a five-dimensional column vector of ones, and $\theta_{y,t}$ is a common unobserved state variable among the five-dimensional waves of the survey-based unemployed labour force, and it represents the Dutch unemployment itself. As such, it is our variable of interest, and as unobserved component, it is assumed to be unknown and estimable. The reason why the unemployment is re-estimated by means of a state space model, using the GREG estimates as observed series, is because the latter are considered too volatile to produce sufficiently reliable monthly estimates for the unemployed labour force at monthly frequency. The additional estimation method via state space models, which was originally proposed by Pfeffermann (1991), improves the precision of the monthly estimates for the unemployment with sample information from previous periods, and can therefore be seen as a form of small area estimation (Rao and Molina, 2015).

The state variable of interest, $\theta_{y,t}$, is assumed to be composed of a trend and a seasonal component (which means that strictly speaking $\theta_{y,t}$ is the sum of state variables, but for simplicity we refer to it as state variable throughout the paper):

$$\theta_{y,t} = L_{y,t} + S_{y,t}.$$

The exclusion of an innovation term in the formula above is motivated by Bollineni-Balabay et al. (2017). The transition equations for the level ($L_{y,t}$) and the slope ($R_{y,t}$) of the trend are, respectively:

$$L_{y,t+1} = L_{y,t} + R_{y,t},$$
$$R_{y,t+1} = R_{y,t} + \eta_{R,y,t}, \quad \eta_{R,y,t} \sim N\left(0, \sigma^2_{R,y}\right).$$

The random walk specification for the slope means that the latter is assumed to be integrated of order 1, I(1), which implies that its first differences are assumed to be stationary (i.e., mean-reverting). Consequently, the level of the trend, which is expressed as the cumulative sum of the slope, is integrated of order 2, I(2), implying that its second differences are stationary. The absence of an innovation term for the trend's level is motivated in van den Brakel and Krieg (2016) as being the result of Likelihood Ratio testing, and implies a smoothness assumption on the level of the unemployment's trend.

The trigonometric stochastic seasonal component allows for the seasonality to vary over

time, and it is modeled as in Durbin and Koopman (2012, Chapter 3):

$$
\begin{aligned}
S_{y,t} &= \sum_{l=1}^{6} S_{1,y,l,t}, \\
\begin{pmatrix} S_{1,y,l,t+1} \\ S_{2,y,l,t+1} \end{pmatrix} &= \begin{bmatrix} \cos(h_l) & \sin(h_l) \\ -\sin(h_l) & \cos(h_l) \end{bmatrix} \begin{pmatrix} S_{1,y,l,t} \\ S_{2,y,l,t} \end{pmatrix} + \begin{pmatrix} \eta_{1,\omega,y,l,t} \\ \eta_{2,\omega,y,l,t} \end{pmatrix}, \\
\begin{pmatrix} \eta_{1,\omega,y,l,t} \\ \eta_{2,\omega,y,l,t} \end{pmatrix} &\sim N\left(0, \sigma^2_{\omega,y} I_2\right),
\end{aligned}
$$

where $h_l = \frac{\pi l}{6}$, for $l = 1, \ldots, 6$, and I_2 is a 2×2 identity matrix.

Rotating panel designs can induce Rotation Group Bias (RGB), i.e., systematic differences among the observations in the subsequent waves (Bailar, 1975). van den Brakel and Krieg (2015) argue that, for the Dutch LFS, the estimates for the unemployment based on the first wave are systematically larger compared to the estimates based on the follow-up waves. Some of the reasons that trigger this phenomenon are discussed in Schiavoni et al. (2021), and they suggest that the answers from the first wave of interviews have to be considered as being the most reliable ones and not to be affected by the RGB. The five-dimensional state vector λ_t in equation (2.1) accounts for the RGB in the second to fifth wave, as proposed in Pfeffermann (1991), and its last four elements are modeled as a random walk because they are supposed to capture the time-dependent differences with respect to the first wave:

$$
\begin{aligned}
&\lambda_{1,t+1} = 0, \\
&\lambda_{j,t+1} = \lambda_{j,t} + \eta_{\lambda,j,t}, \quad \eta_{\lambda,j,t} \sim N\left(0, \sigma^2_{\lambda}\right), \quad j = 2, \ldots, 5.
\end{aligned}
$$

Notice that $\lambda_{1,t+1} = 0$ because it is assumed that the first wave is not affected by the RGB.

The rotating panel design also induces autocorrelation among the survey errors in the follow-up waves. In order to account for this autocorrelation, the survey errors, which are represented by the five-dimensional vector e_t in equation (2.1), are treated as state variables. The transition equation for the survey errors takes the following form:

$$
\begin{aligned}
&e_{j,t} = c_{j,t}\xi_{j,t}, \quad c_{j,t} = \sqrt{\text{var}\left(y_{j,t}\right)}, \quad j = 1, \ldots, 5, \\
&\xi_{1,t+1} \sim N\left(0, \sigma^2_{v_1}\right), \\
&\xi_{j,t+1} = \delta\xi_{j-1,t-2} + v_{j,t}, \quad v_{j,t} \sim N\left(0, \sigma^2_{v_j}\right), \quad j = 2, \ldots, 5, \quad |\delta| < 1, \\
&\text{var}\left(\xi_{j,t}\right) = \sigma^2_{v_j} / \left(1 - \delta^2\right), \quad j = 2, \ldots, 5.
\end{aligned}
$$

The survey errors of all waves, $e_{j,t}$, are assumed to be proportional to the standard errors of the GREG estimates, $\sqrt{\text{var}\left(y_{j,t}\right)}$, for $j = 1, \ldots, 5$, in order to account for heterogeneity in their variances, which are caused by, for instance, changing sample sizes over time. The scaled sampling errors $\xi_{j,t}, j = 1, \ldots, 5$, capture the serial autocorrelation induced by the sampling overlap of the rotating panel. Since in the first wave of interview samples are observed for the first time, the survey errors of the first wave are not autocorrelated with survey errors of previous periods. The survey errors of the second to fifth wave are, instead, correlated with the survey errors of the previous

wave three months before. For this reason van den Brakel and Krieg (2009), following an approach proposed by Pfeffermann et al. (1998), suggest to model the survey errors with an auto-regressive process of order 3, AR(3), without including the first and second lag.

In order to achieve more accurate estimates, or forecasts, of the unemployment, it is possible to augment the model with auxiliary series that are related to this variable. Harvey and Chung (2000), van den Brakel and Krieg (2016) and Schiavoni et al. (2021) show that including in the model the univariate auxiliary series of monthly claimant counts, which represents the number of people claiming unemployment benefits and which is a registry source, can significantly improve the accuracy of estimation (and nowcast) of the unemployment. Only unemployed people who have worked enough time, and therefore paid enough taxes, can receive unemployment benefits in the Netherlands, for a maximum of three years and two months, despite being employed or not, at the end of this period. The claimant counts therefore tend to underestimate the Dutch long-term unemployment. Figure 2.1 displays the monthly time series of the GREG estimates and the claimant counts, from January 2004 until March 2020. It is possible to see how the two series overall tend to follow the same trend over time, but deviate from each other between 2010 and 2016.

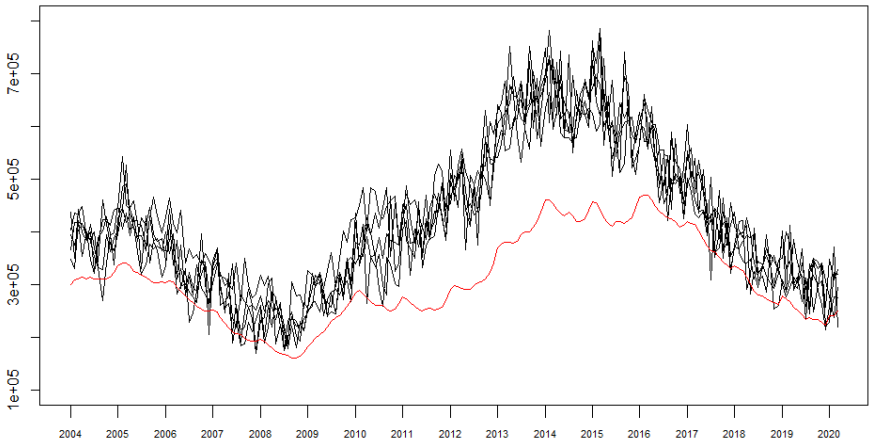

Figure 2.1 Monthly GREG estimates for the Dutch unemployment based on the labour force survey (black), y_t, and the univariate time series of claimant counts in the Netherlands (red).

If we let $x_{CC,t}$ be the univariate series of monthly claimant counts, the labour force model augmented with this auxiliary series, looks as follows:

$$\begin{pmatrix} y_t \\ x_{CC,t} \end{pmatrix} = \begin{pmatrix} 1_5\theta_{y,t} \\ \theta_{CC,t} \end{pmatrix} + \begin{pmatrix} \lambda_t \\ 0 \end{pmatrix} + \begin{pmatrix} e_t \\ \varepsilon_{CC,t} \end{pmatrix}, \quad \varepsilon_{CC,t} \sim N\left(0, \sigma^2_{\varepsilon,CC}\right), \tag{2.2}$$

$$\begin{pmatrix} \theta_{y,t} \\ \theta_{CC,t} \end{pmatrix} = \begin{pmatrix} L_{y,t} \\ L_{CC,t} \end{pmatrix} + \begin{pmatrix} S_{y,t} \\ S_{CC,t} \end{pmatrix}, \tag{2.3}$$

$$\begin{pmatrix} L_{y,t+1} \\ L_{CC,t+1} \end{pmatrix} = \begin{pmatrix} L_{y,t} \\ L_{CC,t} \end{pmatrix} + \begin{pmatrix} R_{y,t} \\ R_{CC,t} \end{pmatrix}, \tag{2.4}$$

$$\begin{pmatrix} R_{y,t+1} \\ R_{CC,t+1} \end{pmatrix} = \begin{pmatrix} R_{y,t} \\ R_{CC,t} \end{pmatrix} + \begin{pmatrix} \eta_{R,y,t} \\ \eta_{R,CC,t} \end{pmatrix}, \tag{2.5}$$

with

$$\text{cov}\begin{pmatrix} \eta_{y,R,t} \\ \eta_{CC,R,t} \end{pmatrix} = \begin{bmatrix} \sigma^2_{R,y} & \rho\sigma_{R,y}\sigma_{R,CC} \\ \rho\sigma_{R,y}\sigma_{R,CC} & \sigma^2_{R,CC} \end{bmatrix}. \tag{2.6}$$

The augmented state space model above shows that the series of claimant counts is also supposed to be composed of a level and a seasonal component, which are assumed to have the same transition equations of the level and the seasonal components of $\theta_{y,t}$.

The static parameters (which are also referred to as "hyperparameters" in the state space literature) and the state variables of the model defined by equations (2.2)-(2.6) are estimated, respectively, by maximum likelihood using the Broyden–Fletcher–Goldfarb–Shanno (BFGS) optimisation algorithm, and by the Kalman filter (details about these estimation methods are provided in Section 3). A diffuse initialisation of the Kalman filter is used for all state variables of the model, except for the 13 state variables that define the autocorrelation structure of the survey errors, for which we use the exact initialisation of Bollineni-Balabay et al. (2017).

The transition equation (2.5) implies that the trend's slopes of the survey-based and the claimant counts series have the same order of integration: they are both I(1). Their innovations are allowed to be correlated, as their covariance matrix in equation (2.6) shows. Harvey and Chung (2000) show, via simulations, that if the magnitude of this correlation parameter is large, there are gains in the accuracy of estimation and nowcast, respectively in terms of MSE and MSFE, of the Kalman filter estimators of $\theta_{y,t}$, $L_{y,t}$ and $R_{y,t}$. In the special case where the absolute value of the correlation parameter is equal to 1, the covariance matrix of equation (2.6) is not full rank any more, which means that the corresponding state variables have the same source of error, and are said to be cointegrated. This correlation parameter is of key importance in our study, because it represents the mean for the Dutch labour force model to exploit auxiliary information.

Notice that the smooth trend model specification for the claimant counts' trend implies that the claimant counts series is I(2).

We employ the method proposed by Harvey and Chung (2000) in order to incorporate auxiliary information in the model, by augmenting the observed series with the auxiliary one. Alternatively, the claimant counts series could be added as a regressor in the measurement equation. However, with this latter option the main part of the unemployment's trend would be explained by the auxiliary series, and its filtered estimates would contain a residual trend instead of the unemployment's trend. Since trend estimates are published as part of the monthly official labour force figures, this approach is not an option for Statistics Netherlands, and we do not consider it in this paper.

Model (2.1) has been used by Statistics Netherlands since 2010 for the production of official labour force figures. To further improve the precision of the time series model estimates, Statistics Netherlands decided in 2014 to augment this model with the series

of Dutch claimant counts. Until the end of 2014, survey-based and auxiliary series were actually cointegrated. In February 2015, some changes were implemented in the registration of claimant counts. Namely, since then people that find a job can receive unemployment benefits up to two months after having found the job. These people are therefore still part of the claimant counts for those two additional months despite being actually employed. This resulted in systematic higher time series estimates for the unemployed labour force in the second quarter of 2015, compared to the model without claimant counts. It was anticipated that this legislative change disturbed the relationship between the survey-based and the claimant counts series, and that a model assuming a time constant correlation incorrectly did not not observe the drop in this parameter during the first months after the legislative change. As a result, Statistics Netherlands went back to the model without claimant counts in June 2015, and revised the monthly figures that were published from March until May 2015. This model has been used for publishing official monthly figures about the Dutch labour force since then. Hence the main purpose of this paper to model the relationship between survey-based and auxiliary series as time-varying, by proposing a method for the estimation of time-varying state correlations in state space models. The correlation parameter in the covariance matrix of equation (2.6) is therefore, hereinafter, assumed to be time-varying.

3 Method for the estimation of a time-varying state correlation

This section describes our proposed approach to model a time-varying state correlation, when this is assumed to be random. For sake of generality, the auxiliary series included in the model will be indicated as x_t (which in the case of the claimant counts is just a scalar). Additionally, we need to impose a restriction on the space of ρ_t, namely of being between -1 and 1. We therefore re-parametrise the correlation parameter as

$$\rho_t = \tanh(\gamma_t),$$

for $t = 1, \dots, T$, and where tanh is the hyperbolic tangent, which is a time-invariant, continuous, invertible, and twice differentiable function.

We let $z_t = (y_t', x_t')'$ be the $n \times 1$ vector that collects all observed series, and $Z_{t-1} = \{z_1, \dots, z_{t-1}\}$ be the available information set at time t. The Dutch labour force model (2.2)-(2.6) can be compactly written as

$$\begin{aligned} z_t &= Z\alpha_t + M\varepsilon_t, \quad \varepsilon_t \sim N(0, H) \\ \alpha_{t+1} &= T\alpha_t + R\eta_t, \quad \eta_t \sim N(0, Q_t), \end{aligned} \tag{3.1}$$

for $t = 1, \dots, T$, where T is the sample size, α_t is the $p \times 1$ vector of state variables and η_t is the corresponding $r \times 1$ vector of disturbances. The respective covariance matrix, Q_t, is varying over time because it contains the time-varying correlation parameter, ρ_t. The $p \times p$ matrix T defines the dynamic structure of the state variables, and R is a $p \times r$ selection matrix. The $n \times p$ matrix Z links the observed series to the state vector, ε_t is

the $q \times 1$ disturbance vector of the observation equation, with covariance matrix H, and M is a $n \times q$ selection matrix. We assume the matrices Z, M, H, T and R to be non-stochastic[2]. If we also assume Q_t to be non-stochastic, which happens if ρ_t is actually constant, or if we assume a deterministic specification that captures the time-variation of ρ_t, then the state space model (3.1) is linear. We indicate with β the vector of unknown time-constant parameters of the linear model (which are contained in the above-listed matrices). Then, conditionally on the information set and β, the observations and the state vector are Gaussian: $z_t|Z_{t-1};\beta \sim N(Za_t, F_t)$ and $\alpha_t|Z_{t-1};\beta \sim N(a_t, P_t)$. Therefore, the log-likelihood function for z_t takes the form[3]

$$\ell = \sum_{t=1}^{T} \ell_t, \tag{3.2}$$

with

$$\ell_t = \log p(z_t|Z_{t-1};\beta) = -\frac{n}{2}\log(2\pi) - \frac{1}{2}\log(\det F_t) - \frac{1}{2}v_t' F_t^{-1} v_t, \tag{3.3}$$

for $t = 1, \dots, T$, where the prediction error v_t and its covariance matrix F_t are evaluated by the following Kalman Filter recursions:

$$\begin{aligned} v_t &= z_t - Za_t & \qquad P_{t|t} &= P_t - P_t Z' F_t^{-1} Z P_t \\ F_t &= ZP_tZ' + MHM' & a_{t+1} &= Ta_t + K_t v_t \\ K_t &= TP_tZ'F_t^{-1} & P_{t+1} &= TP_t(T - K_tZ)' + RQ_tR', \\ a_{t|t} &= a_t + P_tZ'F_t^{-1}v_t \end{aligned} \tag{3.4}$$

for $t = 1, \dots, T$. The vector $a_{t|t}$ represents the filtered estimate of α_t, and $P_{t|t}$ is its estimated covariance matrix. The one-step-ahead prediction of the state vector, together with its predicted covariance matrix, are instead represented, respectively, by a_{t+1} and P_{t+1}. Assuming normality of the innovations is standard in state space models because it allows to estimate β by maximising the log-likelihood (3.2). Under the normality assumption, the Kalman filter yields the minimum variance unbiased estimator of the state vector. However, if the Gaussianity of the innovations is not met,

[2] The exact expressions for all these matrices in the extended Dutch labour force model, can be found in Schiavoni et al. (2021).

[3] In case of a diffuse initialisation of the Kalman filter, we employ the following diffuse log-likelihood (Harvey, 1989), instead of equations (3.2)-(3.3):

$$\ell_d = -\frac{Tn}{2}\log(2\pi) - \frac{1}{2}\sum_{t=d+1}^{T}\left[\log(\det F_t) - \frac{1}{2}v_t' F_t^{-1} v_t\right],$$

with d being the number of nonstationary state variables of the target observed series (in the empirical application of Section 5, d is the number of unobserved components of the GREG estimates for which a diffuse initialisation is used).

then the Kalman filter still provides the minimum variance *linear* unbiased estimator of the state vector, as long as the model is linear (Durbin and Koopman, 2012, Chapter 4).

The correlation parameter, ρ_t, can be assumed to be stochastic, instead of deterministic, by treating γ_t as an additional state variable with its own transition equation:

$$\gamma_{t+1} = \gamma_t + \eta_{\gamma,t}, \quad \eta_{\gamma,t} \sim N\left(0, \sigma_\gamma^2\right) \tag{3.5}$$

for $t = 1, \dots, T$. The state vector hence becomes $\alpha_t^* = (\alpha_t', \gamma_t)'$, yielding what we refer to as the "nonlinear state space model":

$$\begin{aligned} z_t &= Z^* \alpha_t^* + M\varepsilon_t, \quad \varepsilon_t \sim N(0, H) \\ \alpha_{t+1}^* &= T^* \alpha_t^* + R^* \eta_t^*, \quad \eta_t^* \sim N(0, Q_t^*), \end{aligned} \tag{3.6}$$

for $t = 1, \dots, T$, where $\eta_t^* = (\eta_t', \eta_{\gamma,t})'$, and Z^*, T^*, R^* and Q_t^* are straightforwardly obtained by adding γ_t as additional state variable and $\eta_{\gamma,t}$ as additional state innovation. We let τ be the parameter vector that collects all the static parameters of the nonlinear model, i.e., the time-constant parameters appearing in H, T^*, and Q_t^* (including σ_γ) of model (3.6). Notice that the matrices M and H are the same as the ones specified for the linear state space model (3.1). Model (3.6) is nonlinear in its transition equation. To see this, let us define with $C_{Q,t}$ the Cholesky decomposition of Q_t^* (i.e., such that $C_{Q,t} C_{Q,t}' = Q_t^*$). Then $\eta_t^* \sim N(0, Q_t^*)$ can be re-written as $C_{Q,t}\eta_t^* \sim N(0, I_{r+1})$, where $C_{Q,t}\eta_t^*$ involves multiplications (i.e., nonlinear structures) of random components (ρ_t and η_t). This implies that the state vector of the nonlinear model, α_t^*, cannot be estimated by the standard Kalman filter recursions (3.4), and the consequent evaluation of the log-likelihood (3.2) is therefore precluded. As already mentioned in the Introduction, we solve this problem by proposing an indirect inference approach, which makes use of cubic splines for the auxiliary model, in order to estimate τ, and then estimating the state vector, α_t^*, with the Rao-Blackwellised Bootstrap filter (RBBF). The next two sub-sections explain our proposed methodology in detail.

3.1 Indirect inference with a cubic splines approximate model

When the likelihood function needed to estimate the static parameters of a model is intractable, which, as explained above, is the case for a nonlinear state space model, Gourieroux et al. (1993) propose to indirectly estimate these parameters via the optimisation of an "incorrect criterion". This can be, for instance, the exact log-likelihood of an approximate model, which can therefore be easily estimated. In our case a natural approximate model would be a linear Gaussian state space model, which assumes a deterministic specification for the time-varying correlation. We do so by means of cubic splines.

Cubic splines are continuous piecewise polynomial functions of cubic order whose function values and first and second derivatives agree at the points where they join (Smith, 2008). The abscissas of these joint points are called knots and are chosen to determine the complexity of the approximation. A common choice is to set the knots to evenly partition the support $1, \dots, T$ of t. Specifically, in the Monte Carlo simulation and empirical studies, we specify two choices for the location of the knots: at the quartiles and septiles of the sample size. We then let an information criterion decide on the best

choice of knots' location[4]. If the date of a structural change in the time-varying parameter is known, it can be used as (additional) knot. The polynomial order controls for the smoothness of the splines and is treated as fixed (Hansen, 2019).

The deterministic time-varying specification for γ_t, based on cubic splines, is

$$\gamma_t = w_t'\phi, \tag{3.7}$$

where w_t is a $k \times 1$ vector of known weights, which depends on t, on the position of the knots and the distance between them; it corresponds to the t^{th} row of a $T \times k$ matrix W of splines weights constructed as in Poirier (1973), where k is equal to the number of knots. Moreover, ϕ is a $k \times 1$ vector of coefficients. Each element ϕ_j of ϕ, represents the value of γ_t at the j^{th} knot, for $j = 1, \dots, k$. We use a natural cubic spline which restricts the spline functions to be linear beyond the boundary knots, in order to decrease the large variance that affects cubic splines at the boundaries, while paying the price for a larger bias (Hastie et al., 2009, Chapter 5). Notice that the weights w_t make sure that γ_t varies over time, but they are all pre-specified, which means that there is no stochastic component in specification (3.7). This makes sure that the state space model remains linear. Equations (3.1) and (3.7) define what we refer to as the "approximate/auxiliary model" or the "cubic splines model". The parameter vector β of this approximate linear model therefore contains the time-constant parameters appearing in H, T, and Q_t of model (3.1), together with ϕ. Vectors β and τ only differ because the latter contains σ_γ instead of ϕ. Very importantly, β is easily estimated by maximising the log-likelihood (3.2). We indicate with $\hat{\beta}$ the maximum likelihood estimate of β. The cubic splines estimate for ρ_t is therefore equal to $\hat{\rho}_{\text{CS},t} = \tanh(w_t'\hat{\phi})$.

In the context of state space models, a cubic splines approach to estimate time-varying parameters has already been employed by Koopman et al. (2006) and Proietti and Hillebrand (2017). They use this method to model, respectively, time-changing volatilities and smoothly changing parameters over the seasons of the year.

After β has been estimated by maximum likelihood on the observed series, Z_T, the indirect inference approach proceeds by simulating, for a given value of τ, S paths of Z_T according to the nonlinear model. The nonlinear model is therefore required to be simulable (which is the case for model (3.6)). The cubic splines model is re-estimated on every simulated path $Z_T^{(s)}(\tau)$, for $s = 1, \dots, S$, yielding S different maximum likelihood estimates, $\hat{\beta}^{(s)}(\tau)$. The parameter vector of the nonlinear model, τ, is then estimated as

$$\hat{\tau} = \underset{\tau \in \mathcal{T}}{\operatorname{argmin}} \left(\hat{\mu} - \frac{1}{S}\sum_{s=1}^{S} \hat{\mu}^{(s)}(\tau) \right)' \left(\hat{\mu} - \frac{1}{S}\sum_{s=1}^{S} \hat{\mu}^{(s)}(\tau) \right), \tag{3.8}$$

[4] The information criteria that we employ are the Akaike and the Bayesian, respectively given by the following expressions (Durbin and Koopman, 2012, Chapter 7):

$$\text{AIC} = \frac{1}{T}\left[-2\ell_d + 2\,(d + \dim(\beta))\right]$$

$$\text{BIC} = \frac{1}{T}\left[-2\ell_d + \log(T)\,(d + \dim(\beta))\right],$$

where $\dim(\beta)$ is the dimension of β. We use the former criterion in the Monte Carlo simulation study of Section 4, and the latter in the empirical application of Section 5.

where $\mathcal{T}$ is the parameter space of τ. The vector $\hat{\mu} = \left(\hat{\beta}_{\setminus\hat{\phi}}, (\hat{\phi})\right)$, where $\hat{\beta}_{\setminus\hat{\phi}}$ corresponds to the vector $\hat{\beta}$ without $\hat{\phi}$, and $(\hat{\phi}) = \frac{1}{k-1}\sum_{j=1}^{k}(\hat{\phi}_j - \bar{\hat{\phi}})^2$ is the variance of $\hat{\phi}$, with $\hat{\phi}_j$ being its j^{th} element and $\bar{\hat{\phi}} = \frac{1}{k}\sum_{j=1}^{k}\hat{\phi}_j$. In the literature about indirect inference, the minimisation (3.8) is generally applied to $\hat{\beta}$ directly[5], instead of a modified version of it, which in our case is $\hat{\mu}$. However, in our setting matching the estimates for ϕ, based on true and simulated data, is inadvisable since this parameter vector bears information about the evolution of γ_t over time, not only about σ_γ, which we instead aim at estimating by indirect inference. The goal at this stage is to only estimate the time-constant parameters of the nonlinear model, not the evolution of its state variables over time, which we instead need in the filtering step (described in Section 3.2). This is the reason why the simulated paths, $Z_T^{(s)}(\tau)$, only need to depend on the values of τ and need not be conditioned on the observed data, Z_T; the maximum likelihood estimates for ϕ can be very different for distinct simulated paths, even if these paths are generated based on the same value of τ, and therefore of σ_γ. We therefore need a measure which is a function of $\hat{\phi}$, but that is informative only about σ_γ; the statistics $(\hat{\phi})$ achieves this goal since $\hat{\phi}_j$ represents the value of the cubic splines estimate of γ_t at the j^{th} knot, for $j = 1, \dots, k$, and $(\hat{\phi})$ is therefore a measure of the cubic splines estimate's spread. Intuitively, the larger σ_γ, the more volatile we would expect the cubic splines estimate of γ_t to be, and therefore the larger the value of $(\hat{\phi})$[6].

Finally, notice that $\dim(\mu) \geq \dim(\tau)$, in order for τ to be idenitifiable (Gourieroux et al., 1993). In our case the two vectors have the same dimension[7].

Algorithm 1 reports the detailed steps for the implementation of the indirect inference estimation of τ.

We conclude this sub-section by remarking that other non-random time-varying specifications, than the one based on cubic splines, could potentially be used for the approximate model in the indirect inference approach. For instance, we also followed the idea of Delle Monache et al. (2016), who estimate time-varying parameters in state space models with the score-driven method of Creal et al. (2013) and Harvey (2013), by assuming that the time-varying correlation depends on its past values and past values of the score function (i.e., the scaled derivative of the log-likelihood with respect to the correlation). Nevertheless, Monte Carlo simulations' results, which we do not report in this paper, show that this method does not satisfactorily estimate the time-varying correlation. Moreover, this approach is computationally much more expensive than the one based on cubic splines. We therefore decided to not pursue it.

5) In this case Gourieroux et al. (1993) show that $\hat{\tau}$ is a consistent estimator of τ, and that, for S fixed, $\sqrt{T}\,(\hat{\tau} - \tau)$ is asymptotically normally distributed with covariance matrix depending on the function relating β and τ, which is (as in our case) often unknown.

6) Monte Carlo simulations' results, that we do not report in this paper, suggest that other measures, such as the variance of the cubic splines estimate of γ_t, can alternatively be employed in order to achieve the same goal.

7) We choose a random walk specification for γ_t, given in equation (3.5), because it is a rather flexible one, and it allows for structural changes in the correlation parameter. Generally, an AR(1) specification could be employed instead. However, in the latter case the inequality would not hold anymore, because the AR(1) specification implies that at least one additional parameter in the nonlinear model needs to be estimated.

Algorithm 1 INDIRECT INFERENCE ESTIMATION OF τ

1: Estimate the cubic splines model on the observed data, Z_T, by Kalman filter and maximum likelihood. Store the maximum likelihood estimate, $\hat{\beta}$.
2: Generate standard normal errors $\tilde{\varepsilon}_t^{(s)} \sim N(0, I_q)$, and $\tilde{\eta}_t^{(s)*} \sim N(0, I_{r+1})$, for $t = 1, \dots, T$ and $s = 1, \dots, S$. These simulated errors are used for *all* values of τ in minimisation (3.8), which means that they have to be stored *before* performing the minimisation (otherwise the objective function used in equation (3.8) is not continuous with respect to τ).
3: **for** $\tau \in \mathcal{T}$ **do**
4: **for** $s \in \{1, \dots, S\}$ **do**
5: Set initial values $\alpha_0^{(s)*} = 0$. Then generate new series $Z_T^{(s)}$ according to the nonlinear model (3.6). This is done as follows:
6: **for** $t \in \{1, \dots, T\}$ **do**
7: Let C_H be the Cholesky decomposition of H. Get $\varepsilon_t^{(s)} = C_H \tilde{\varepsilon}_t^{(s)}$.
8: Get $\eta_{\gamma,t}^{(s)} = \sigma_\gamma \tilde{\eta}_{\gamma,t}^{(s)}$, and then $\gamma_t^{(s)} = \gamma_{t-1}^{(s)} + \eta_{\gamma,t}^{(s)}$.
9: Evaluate $Q_t^{(s)*}$ at $\gamma_t^{(s)}$. Let $U_{Q,t}^{(s)}$ be the Cholesky decomposition of $Q_t^{(s)*}$ without its last row and column (which is $Q_t^{(s)}$). Get $\eta_t^{(s)} = U_{Q,t}^{(s)} \tilde{\eta}_t^{(s)}$ (notice that $\tilde{\eta}_t^{(s)}$ is equal to $\tilde{\eta}_t^{(s)*}$ without its last element, which is $\tilde{\eta}_{\gamma,t}^{(s)}$).
10: Get $\alpha_t^{(s)} = T\alpha_{t-1}^{(s)} + R\eta_t^{(s)}$.
11: Get $z_t^{(s)} = Z\alpha_t^{(s)} + M\varepsilon_t^{(s)}$.
12: **end for**
13: Let $Z_T^{(s)} = \{z_1^{(s)}, \dots, z_T^{(s)}\}$. Estimate the cubic splines model on the simulated data, $Z_T^{(s)}$, by Kalman filter and maximum likelihood. Store the maximum likelihood estimate, $\hat{\beta}^{(s)}$, and respective $\hat{\mu}^{(s)}$.
14: **end for**
15: Store $\left(\hat{\mu} - \frac{1}{S}\sum_{s=1}^{S} \hat{\mu}^{(s)}\right)' \left(\hat{\mu} - \frac{1}{S}\sum_{s=1}^{S} \hat{\mu}^{(s)}\right)$.
16: **end for**
17: Find the value of τ which minimises $\left(\hat{\mu} - \frac{1}{S}\sum_{s=1}^{S} \hat{\mu}^{(s)}\right)' \left(\hat{\mu} - \frac{1}{S}\sum_{s=1}^{S} \hat{\mu}^{(s)}\right)$. This can be done for a grid of values of τ, or, more appropriately, with a gradient/Hessian-based optimisation algorithm that finds the solution numerically.
Notice that, for notation simplicity, in the algorithm we omitted the dependence on τ of all simulated series and respective maximum likelihood estimates. However, it should be kept in mind that all elements with an (s)-superscript depend on τ.

3.2 Rao-Blackwellised bootstrap filter

Once the static parameters of the nonlinear model have been estimated, we can proceed with the filtering step in order to estimate ρ_t, together with the other state variables of the model. The nonlinearity of the state space model remains also after the estimation of τ, which means that alternative filters than the Kalman filter, need to be used. As already anticipated in the Introduction, we employ the bootstrap filter of Gordon et al. (1993), which is a type of particle filter.

Before proceeding with the explanation of the method, we point out that the bootstrap filter is always applied to the nonlinear model (3.6), evaluated at the indirect inference estimate, $\hat{\tau}$, even when we do not make this explicit in what follows. We therefore indicate with $\hat{T}^*$, $\hat{H}$, and $\hat{Q}_t^*$ the indirect inference estimates for the corresponding

matrices of model (3.6). Notice that $\hat{Q}_t$ (from model (3.1)) is equivalent to $\hat{Q}_t^*$ without its last row and column.

The idea of bootstrap filtering is to simulate, at time t and unconditionally on the data, z_t, M values for each state variable of model (3.6), from the density distribution implied by their transition equation: $\alpha_t^{(m)*} \sim N\left(\hat{T}^* \alpha_{t-1}^{(m)*}, R^* \hat{Q}_t^* R^{*\prime}\right)$, for $m = 1, \dots, M$. These M generated values are called particles. Of course, since the particles are simulated unconditionally on the data, some of them will be far from the true values of the state variables, and some other will be close. To make sure that the latter happens, M should be large. In order to understand which of the particles are closer to the true values, we compute the likelihood for each one of them: $p\left(z_t|\alpha_t^{(m)*}, \hat{\tau}\right)^{(m)}$, for $m = 1, \dots, M$. The larger the likelihood, the more likely the corresponding particle is close to the true value of α_t^*. We then build M weights that are proportional to the respective likelihoods, $\tilde{w}_t^{(m)} = w_{t-1}^{(m)} p\left(z_t|\alpha_t^{(m)*}, \hat{\tau}\right)^{(m)}$, and we standardise them: $w_t^{(m)} = \frac{\tilde{w}_t^{(m)}}{\sum_{m=1}^{M} \tilde{w}_t^{(m)}}$, for $m = 1, \dots, M$. Finally, we resample with replacement M particles with probabilities corresponding to the normalised weights $\left\{w_t^{(1)}, \dots, w_t^{(M)}\right\}$, in order to make sure that we keep the particles that yield a larger likelihood. The bootstrap filter estimate for α_t^* at time t is equal to $\frac{1}{M}\sum_{m=1}^{M} \alpha_t^{(m)*}$, where $\alpha_t^{(m)*}$, for $m = 1, \dots, M$, are the resampled particles. These resampled particles are then used at time $t+1$ in the expected value of the normal distribution from which new M vectors $\alpha_{t+1}^{(m)*}$ are generated. The entire procedure then repeats again until $t = T$.

However, we do not stop at standard bootstrap filtering because when the state vector is large, which is the case for the extended Dutch labour force model, then the bootstrap filter can become computationally costly. We therefore notice that if γ_t is known at time t, then model (3.6) becomes linear again, as it is only γ_t that triggers the nonlinearity of the model. Therefore, if we could condition on γ_t at time t, then the other state variables, α_t, could be predicted by standard Kalman filtering, which is a very efficient estimation method. This conditioning can be achieved by Rao-Blackwellising the bootstrap filter, as proposed by Chen and Liu (2000). Namely, at time t we generate M particles only for γ_t: $\gamma_t^{(m)} \sim N\left(\gamma_{t-1}^{(m)}, \hat{\sigma}_\gamma\right)$, for $m = 1, \dots, M$. Then the one-step ahead forecasts of the other state variables, $a_{t+1}^{(m)}$, together with their variances, $P_{t+1}^{(m)}$, can be obtained by running the prediction step of the Kalman filter recursions (3.4), applied to the linear model (3.1) evaluated at $\hat{\tau}$ and with γ_t replaced by $\gamma_t^{(m)}$.

At time $t+1$, for each set of particles $\left\{\gamma_t^{(m)}, a_{t+1}^{(m)}, P_{t+1}^{(m)}\right\}$, it is then possible to obtain the prediction error, $v_{t+1}^{(m)}$, together with its covariance matrix, $F_{t+1}^{(m)}$, for $m = 1, \dots, M$. These two elements can be used in order to evaluate the following likelihood:

$$p\left(z_{t+1}|\gamma_t^{(m)}, a_{t+1}^{(m)}, P_{t+1}^{(m)}, \hat{\tau}\right)^{(m)} = \\ = \exp\left(-\frac{n}{2}\log(2\pi) - \frac{1}{2}\log\left(\det F_{t+1}^{(m)}\right) - \frac{1}{2} v_{t+1}^{(m)\prime}\left(F_{t+1}^{(m)}\right)^{-1} v_{t+1}^{(m)}\right), \quad (3.9)$$

for $m = 1, \dots, M$. The M likelihood values can in turn be employed to build the same standardised weights used in the standard bootstrap filter, which allow to resample with replacement the sets of particles $\left\{\gamma_t^{(m)}, a_{t+1}^{(m)}, P_{t+1}^{(m)}\right\}$, for $m = 1, \dots, M$, that yield larger likelihood values. The resampled particles can then be used in order to repeat the

procedure again for the next period in time. Notice that we also need to resample $a_{t+1}^{(m)}$ and $P_{t+1}^{(m)}$ because they need to be used as inputs in the prediction step of the Kalman filter, in order to obtain $a_{t+2}^{(m)}$ and $P_{t+2}^{(m)}$, for $m = 1, \dots, M$. The Rao-Blackwellised bootstrap filter (RBBF) estimate of γ_t at time t, which we indicate with $\hat{\gamma}_{\text{RBBF},t}$, is again obtained by taking the average of the M resampled particles $\gamma_t^{(m)}$. Algorithm 2 outlines the Rao-Blackwellised bootstrap filter estimation of ρ_t in detail.

Some remarks are now in place. First, the likelihood (3.9) for z_t at time t is conditioned on $\gamma_{t-1}^{(m)}$, i.e., on values for the time-varying correlation at the previous point in time. This is due to the Kalman filter recursions (3.4), where the prediction errors, v_t, and respective covariance matrix, F_t, depend on Q_{t-1}, which contains γ_{t-1}, not Q_t. Therefore, it is only possible to obtain the RBBF estimate of γ_t for $t = 1, \dots, T-1$, and not for the last point in time, T. This is a consequence of the Rao-Blackwellisation as this issue does not arise in standard bootstrap filtering. In the latter case all state variables are generated simultaneously, whereas in the former only *predictions* of α_{t+1} can be obtained based on sampled values for γ_t.

Second, the final estimates for the state vector α_t, can be obtained by running the standard Kalman filter recursions (3.4) applied to the linear model evaluated at $\hat{\tau}$ and with γ_t replaced by $\hat{\gamma}_{t,\text{RBBF}}$, for $t = 1, \dots, T-1$ (notice that the estimate for α_t at time T is also unavailable). Although we do not cover it in this paper, we would like to point out that a prediction for γ_T could be obtained, for instance, by taking the *unweighted* (i.e., not depending on likelihood values) average of the M particles $\gamma_T^{(m)}$, which in turn could be employed to predict α_T.

Third, a more efficient particle filter could be obtained by generating particles for γ_t, conditionally on the observed data, z_t. This can be done by, for instance, using a sequential importance sampling approach, instead of the bootstrap filter. However, as pointed out in the Introduction, the type of nonlinearity we are dealing with challenges the quest for an importance density (i.e., a linear model that approximates the nonlinear one, in a more sophisticated way than the cubic splines model), which is needed in order to implement the above-mentioned approach (see Durbin and Koopman (2012, Chapter 12) and Creal (2012) for details about this and other methods).

Fourth, the resampling step of the algorithm is sometimes necessary in order to avoid the degeneracy of the particle filter over time (see again Durbin and Koopman (2012, Chapter 12) and Creal (2012) for an in-depth discussion of this problem). More sophisticated resampling methods, than the generalised one discussed above, can be employed. Li et al. (2015) provide an extensive review of all existing resampling methods for particle filtering. The ones that are shown to yield the particle filters with lowest Monte Carlo variation, are the stratified resampling of Kitagawa (1996) and the residual resampling of Liu and Chen (1998). We employ the former. However, before performing stratified resampling, we include an additional step. As mentioned in the Introduction, the likelihood function for z_t, given in equation (3.9), is not that sensitive to different values of $\gamma_{t-1}^{(m)}$: in other words, the M particles $\gamma_{t-1}^{(m)}$ yield different values for the likelihood, but these differences are not large. Therefore, the corresponding normalised weights are similar to each other and any kind of resampling method will tend to select most of the particles, yielding a final RBBF estimate for γ_t that looks rather constant over time. In order to avoid this problem we first increase the differences among the

normalised weights, which in turn increases the probability of resampling those particles that yield slightly larger likelihood values. We do so by following Chen et al. (2001), who take functions of the normalised weights, $\left[w_t^{(m)}\right]^{p_t}$ for $m = 1, \dots, M$, where $p_t \geq 0$ and depends on the coefficient of variation, which takes the expression

$$CV_t = \left[\frac{1}{M}\sum_{m=1}^{M}\left(Mw_t^{(m)} - 1\right)^2\right]^{0.5},$$

and is a measure of weight instability. It varies between 0 and $\sqrt{M-1}$. If all weights are equal, then CV_t is equal to its lower bound (Creal, 2012). If the goal is to give more presence to the particles with larger weights, which is our case, then $p_t > 1$ if the coefficient of variation is low, otherwise $p_t < 1$. We use $p_t = \ln\left(\frac{\sqrt{M-1}}{CV_t}\right)$ in order to achieve this goal. Once the weights have been transformed according to this function, they have to be re-standardised before performing stratified resampling.

Finally, for simplicity we sometimes state, throughout the paper, that the RBBF is employed to estimate the entire state vector of the nonlinear model. However, it should be now clear that it is really only ρ_t that is estimated by the RBBF, and the remaining part of the state vector is estimated by Kalman filtering with ρ_t replaced by its RBBF estimate. The above-mentioned simplification therefore only helps us to point out that it is the the RBBF that solves the nonlinearity of the model, and that therefore allows us to estimate the state vector.

Algorithm 2 RAO-BLACKWELLISED BOOTSTRAP FILTER ESTIMATION OF ρ_t

1: Initialise the filter at $t = 0$ with $\tilde{w}_0^{(m)} = 1$ (which implies $w_0^{(m)} = 1/M$), for $m = 1, \ldots, M$. First sample $\gamma_0^{(m)} \sim N\left(\hat{\gamma}, \hat{\sigma}_\gamma^2\right)$, where $\hat{\gamma}$ is the maximum likelihood estimate of γ from the model where this parameter is treated as static. Then $a_1 \sim N\left(0, \hat{Q}_0^{(m)}\right)$, and set $P_1^{(m)} = \hat{Q}_0^{(m)}$, for $m = 1, \ldots, M$. In this case a_t is the one-step ahead prediction of the Kalman filter for α_t, with P_t being its predicted covariance matrix, and $\hat{Q}_0^{(m)}$ is evaluated at $\gamma_0^{(m)}$. We need initialisations for both a_t and P_t in order to implement the Kalman filter.

2: **for** $t \in \{1, \ldots, T\}$ **do**

3: Use $\left\{\gamma_{t-1}^{(m)}, a_t^{(m)}, P_t^{(m)}\right\}$ in order to run the prediction step of the Kalman filter applied to the linear model evaluated at $\hat{\tau}$, which yields $v_t^{(m)}$ and $F_t^{(m)}$. Then compute

$$p\left(z_t|\gamma_{t-1}^{(m)}, a_t^{(m)}, P_t^{(m)}, \hat{\tau}\right)^{(m)} = \\ = \exp\left(-\frac{n}{2}\log(2\pi) - \frac{1}{2}\log\left(\det F_t^{(m)}\right) - \frac{1}{2}v_t^{(m)'}\left(F_t^{(m)}\right)^{-1}v_t^{(m)}\right),$$

for $m = 1, \ldots, M$.

4: Compute the weights

$$\tilde{w}_t^{(m)} = w_{t-1}^{(m)} p\left(z_t|\gamma_{t-1}^{(m)}, a_t^{(m)}, P_t^{(m)}, \hat{\tau}\right)^{(m)}$$

for $m = 1, \ldots, M$. Then obtain the normalised weights

$$w_t^{(m)} = \frac{\tilde{w}_t^{(m)}}{\sum_{m=1}^{M}\tilde{w}_t^{(m)}},$$

for $m = 1, \ldots, M$.

5: Resample M particles $\left\{\gamma_{t-1}^{(m)}, a_t^{(m)}, P_t^{(m)}\right\}$, with $m = 1, \ldots, M$, with replacement, based on the modified stratified resampling technique described at the end of Section 3.2

6: Reset $w_t^{(m)} = 1/M$ for $m = 1, \ldots, M$.

7: Compute

$$\hat{\gamma}_{\text{RBBF},t-1} = \frac{1}{M}\sum_{m=1}^{M}\gamma_{t-1}^{(m)},$$

which is the Rao-Blackwellised bootstrap filter estimate for γ_{t-1}. To get the corresponding estimate for ρ_{t-1} we take the hyperbolic tangent of $\hat{\gamma}_{\text{RBBF},t-1}$.

8: Draw $\gamma_t^{(m)} \sim N\left(\gamma_{t-1}^{(m)}, \hat{\sigma}_\gamma^2\right)$ and use it with the resampled particles $\left\{a_t^{(m)}, P_t^{(m)}\right\}$ in order to run the prediction step of the Kalman filter applied to the linear model evaluated at $\hat{\tau}$ and with γ_t replaced by $\gamma_t^{(m)}$, which yields $\left\{a_{t+1}^{(m)}, P_{t+1}^{(m)}\right\}$, for $m = 1, \ldots, M$.

9: **end for**

10: The final estimates for α_t can be obtained by running the usual Kalman filter applied to the linear model evaluated at $\hat{\tau}$ and with γ_t replaced by $\hat{\gamma}_{t,\text{RBBF}}$, for $t = 1, \ldots, T-1$.

4 Monte Carlo simulation study

We conduct a Monte Carlo simulation study to assess the performance of the two estimation methods proposed in Section 3: the cubic splines method, which already is, per se, an estimation method of the time-varying state correlation, and the method based on the combination of indirect inference and Rao-Blackwellised bootstrap filtering. The performance of the methods is evaluated in several ways. First, we want to assess whether the indirect inference approach appropriately estimates the static parameters of the nonlinear model. Secondly, we check if the proposed methods are able to estimate the true time-varying relationships, and, in case, to which level of accuracy. Finally, since in the empirical application our variable of interest, the Dutch unemployment, is assumed to be unknown and therefore enters the model as unobserved component, we want to understand to which extent the accuracy of the estimation of state variables of interest changes if we take the time-varying relationships between observed series into account.

For sake of computational time, in the Monte Carlo simulation study we consider the following bivariate local level model, which is more simple than the Dutch Labour Force model:

$$z_t = Z\alpha_t + \varepsilon_t, \quad \varepsilon_t \sim N(0, H)$$
$$\alpha_{t+1} = T\alpha_t + \eta_t, \quad \eta_t \sim N(0, Q_t), \quad t = 1, \dots, T,$$

where $z_t = (y_t, x_t)'$, $\alpha_t = (L_{y,t}, L_{x,t})'$, ε_t and η_t are all 2×1 vectors, $Z = T = I_2$, $H = \text{diag}(\sigma^2_{\varepsilon,y}, \sigma^2_{\varepsilon,x})$, with $\sigma_{\varepsilon,y} = \sigma_{\varepsilon,x} = 1$, and $Q_t = \begin{bmatrix} \sigma^2_{\eta,y} & \rho_t \sigma_{\eta,y}\sigma_{\eta,x} \\ \rho_t \sigma_{\eta,y}\sigma_{\eta,x} & \sigma^2_{\eta,x} \end{bmatrix}$, with $\sigma_{\eta,y} = \sigma_{\eta,x} = 1$ (we are also implicitly imposing $M = R = I_2$).

In the model above, z_t represents the observed vector, α_t the vector of state variables, ε_t the vector of innovations in the measurement equation, and η_t the vector of innovations in the transition equation. We assume that the state variable of the first observable series, $L_{y,t}$, is the unobserved component of interest.

We consider the following data generating processes (DGPs) for the time-varying parameter, ρ_t, which are partly inspired by Creal et al. (2011) and Delle Monache et al. (2016):

1. Constant: $\rho_t = 0.9$
2. Sine: $\rho_t = 0.5 + 0.4\cos(2\pi t/(T/3))$
3. Fast sine: $\rho_t = 0.5 + 0.4\cos(2\pi t/(T/6))$
4. Step: $\rho_t = 0.9 - 0.5(t > T/2)$
5. Ramp: $\rho_t = 2/T \mod (t/(T/2))$
6. Random walk: $\rho_t = \tanh(\gamma_t)$, where $\gamma_t = \gamma_{t-1} + \eta_{\gamma,t}$, with $\eta_{\gamma,t} \sim N(0, \sigma^2_\gamma)$,

for $t = 1, \dots, T$. We consider two different sample sizes: $T = 200$, which is close to the sample size of our empirical application, and $T = 500$. For the random walk specification of ρ_t, we set $\sigma_\gamma = 0.1$ when $T = 200$ and $\sigma_\gamma = 0.05$ when $T = 500$, to make sure that ρ_t does not become too volatile with a larger sample size (since the variance of a

random walk process increases with time). An improvement in estimation performance is to be expected with a larger sample size. We run $n_{\text{sim}} = 500$ Monte Carlo simulations and always use $S = 3$ simulations for the indirect inference method, and $M = 5000$ particles for the RBBF. We use the BFGS algorithm to solve the minimisation problem, given in equation (3.8), that finds the indirect inference estimates.

We start the discussion of the Monte Carlo simulations' results by looking at the performance of the indirect inference approach in estimating the static parameters of the nonlinear model. Figure 4.1 shows the density distributions of the indirect inference estimators of the elements of $\tau = \left(\sigma_{\eta,y}, \sigma_{\eta,x}, \sigma_{\varepsilon,y}, \sigma_{\varepsilon,x}, \sigma_{\gamma}\right)'$, based on the Monte Carlo replicates, together with the true values of these parameters, when the DGP for ρ_t is a random walk. All distributions are centered around the true values, and their spread decreases with the sample size. For σ_{γ}, the distribution of its indirect inference estimator is skewed to the right and shows a bump around values of the parameter close to zero, which tends to be less pronounced, but does not disappear, with a larger sample size . This issue seems somewhat similar to the pile-up problem discussed, among others, by Shephard and Harvey (1990) and Stock and Watson (1998): if the scale parameter (in our case σ_{γ}) of a coefficient that varies stochastically over time by following a random walk specification, is small, then its maximum likelihood estimator has a point mass at zero, and this probability mass decreases with a larger sample size. The results shown in Figure 4.1 are obtained by using the true values of the parameters as initial values in the BFGS algorithm. In practice, a good starting value for σ_{γ} is difficult to find. Figure A.1 therefore reports the same results when the initial value for σ_{γ} is twice as big as its true one. When $T = 200$, the algorithm gets stuck around the initial value half of the times, making the distribution of the indirect inference estimator of σ_{γ} look bimodal. This problem, however, does not occur anymore when the sample size increases; in this case the distribution is very similar to the one shown in Figure 4.1. We therefore advise practitioners who deal with small sample sizes, to first evaluate the objective function that needs to be minimised in order to find the indirect inference estimates (from equation (3.8)), for a grid of values for σ_{γ}, in order to come up with a good starting value for this parameter (we do so ourselves in the empirical application of Section 5). Figures A.2-A.6 show the same results for the remaining five DGPs of ρ_t. All distributions, for all parameters except σ_{γ}, are again symmetrical and centered around the true values of the parameters, and their spread decreases with the sample size. In these cases, however, we do not know the true value for σ_{γ}, so we cannot assess whether its indirect inference estimator is centered around it. The shapes of the distributions for the latter estimator are similar to the ones observed for the random walk specification of ρ_t. The BFGS algorithm in these cases is initialised at $\sigma_{\gamma} = 0.1$ when $T = 200$ and $\sigma_{\gamma} = 0.05$ when $T = 500$.

Next we investigate the accuracy of our methods in estimating the time varying correlation and whether treating ρ_t as time-varying also improves the estimation of the state variable of interest. We indicate with $\hat{L}_{y,t}$ the Kalman filter estimator (i.e., the first element of $a_{t|t}$ from the Kalman filter recursions (3.4)) of $L_{y,t}$, and with $\hat{\rho}_t$ the estimator of ρ_t (whether this estimator is based on the cubic splines or the RBBF method, will be clear in the discussion that follows). The Mean Squared Error (MSE) and the squared

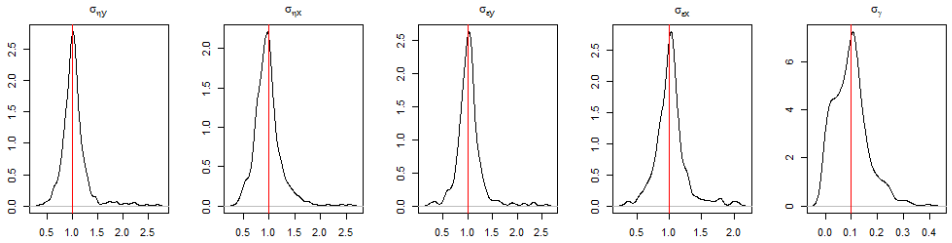

(a) $T = 200$

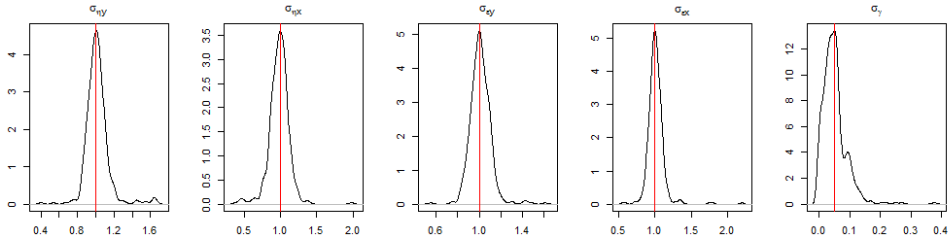

(b) $T = 500$

Figure 4.1 Distribution of the indirect inference estimators of the static parameters of the nonlinear model, $\tau = \left(\sigma_{\eta,y}, \sigma_{\eta,x}, \sigma_{\varepsilon,y}, \sigma_{\varepsilon,x}, \sigma_{\gamma}\right)'$, based on the Monte Carlo replicates, when the DGP of ρ_t is a random walk; $S = 3$, $n_{\text{sim}} = 500$. The red lines represent the true values of the parameters.

bias of $\hat{\rho}_t$ are computed as follows:

$$\text{MSE}\left(\hat{\rho}_t\right) = \frac{1}{T-1-d}\sum_{t=d+1}^{T-1}\left(\frac{1}{n_{\text{sim}}}\sum_{s=1}^{n_{\text{sim}}}\left(\hat{\rho}_{t,s}-\rho_{t,s}\right)^2\right),$$

$$\text{bias}^2\left(\hat{\rho}_t\right) = \frac{1}{T-1-d}\sum_{t=d+1}^{T-1}\left(\frac{1}{n_{\text{sim}}}\sum_{s=1}^{n_{\text{sim}}}\left(\hat{\rho}_{t,s}-\rho_{t,s}\right)\right)^2.$$

The same measures of fit are obtained also for $\hat{L}_{y,t}$ by substituting ρ_t by $L_{y,t}$ in the formulae above ($d = 0$ for the measures of $\hat{\rho}_t$, and $d = 1$ for the measures of $\hat{L}_{y,t}$, since $L_{y,t}$ is the only state variable of the target series which requires a diffuse initialisation). The MSE captures both the variance and the bias of the estimators, and therefore gives an indication (also) of their volatility. The squared bias, instead, is supposed to only capture the difference between the estimated and the true values. We use the square of the bias because we deal with estimators of time-varying parameters/variables, and therefore averaging the biases over time, without taking their squared values, would provide a misleading measure of comparison among different methods. Table 4.1 reports these measures of fit, obtained with both the cubic splines and the RBBF methods, relative to the same measures observed while estimating the correlation as time-constant (i.e., by maximum likelihood). We refer to Table A.1 for the absolute figures. We indicate with "ideal Rao-Blackwellised bootstrap filter" the setting where the static parameter vector τ is not estimated by indirect inference, but it is treated as known (which is only possible when the DGP of ρ_t is a random walk), hence the term "ideal". This should allow us to quantify the influence that the estimation of the static parameters by indirect inference has on the performance of the RBBF. The Tables show that, when $T = 200$, the MSE of $\hat{\rho}_t$ is almost always better when the correlation parameter is estimated as constant, since the other two methods are, because of their

time-varying nature, obviously more volatile. The latter methods, however, tend to strongly beat the time-constant estimation of the correlation in terms of squared bias, indicating that they are able to capture its time-variation (when this is present). The cubic splines shows a better performance than the RBBF, due to its milder volatility, except when the true DGP for ρ_t is a fast sine; the RBBF seems therefore more suited than the cubic splines method in estimating rapidly-changing time variations in the correlation parameter. The ideal RBBF only shows a marginal improvement over the RBBF, suggesting that the estimation of the static parameters by indirect inference does not strongly influence the performance of the filter. All measures of fit for the two methods improve when the sample size increases, also with respect to estimating ρ_t as time-constant. When the true correlation is static, however, estimating it as such is preferred.

	$T = 200$						$T = 500$					
	0.9	Sine	Fast sine	Step	Ramp	Random walk	0.9	Sine	Fast sine	Step	Ramp	Random walk
						Cubic splines						
MSE($\hat{\rho}_t$)	25.769	1.688	2.194	1.269	1.345	0.920	8.114	0.615	1.364	0.454	0.643	0.574
bias^2($\hat{\rho}_t$)	45.540	0.086	1.016	0.069	0.178	0.505	29.112	0.123	1.003	0.062	0.165	0.001
MSE($\hat{L}_{y,t}$)	1.015	1.002	1.015	0.983	0.993	0.982	1.004	0.983	1.003	0.970	1.019	0.988
bias^2($\hat{L}_{y,t}$)	0.948	1.048	0.982	0.948	0.978	0.955	0.997	0.991	0.988	0.953	1.000	1.043
						Rao-Blackwellised bootstrap filter						
MSE($\hat{\rho}_t$)	28.118	1.835	1.716	1.565	1.775	1.269	15.317	1.504	1.207	1.048	1.457	1.074
bias^2($\hat{\rho}_t$)	47.041	0.623	0.845	1.813	0.442	1.191	97.757	0.370	0.878	0.228	0.337	0.003
MSE($\hat{L}_{y,t}$)	1.889	1.121	1.083	1.296	1.236	1.175	1.057	1.074	1.011	1.051	1.087	1.026
bias^2($\hat{L}_{y,t}$)	1.858	1.095	0.991	1.403	1.098	1.030	1.001	1.036	0.995	1.018	1.039	1.063
						Ideal Rao-Blackwellised bootstrap filter						
MSE($\hat{\rho}_t$)						1.183						1.118
bias^2($\hat{\rho}_t$)						1.070						0.002
MSE($\hat{L}_{y,t}$)						0.997						1.004
bias^2($\hat{L}_{y,t}$)						1.017						1.043

Table 4.1 Mean squared error and squared bias for the cubic splines and the Rao-Blackwellised bootstrap filter estimators of ρ_t, and the Kalman filter estimator of $L_{y,t}$, *relative* to the same measures of fit obtained while estimating ρ_t as time-constant. The second row lists the DGPs for ρ_t. "Ideal Rao-Blackwellised bootstrap filter" indicates that the static parameter vector τ is treated as known. $S = 3$, $M = 5000$, $n_{\text{sim}} = 500$.

Since time-variation is the focal point of this paper, it is also interesting to investigate how the two estimation methods perform over time. Figures 4.2 and 4.3 display, for each deterministic DGP of ρ_t, the 5%, 20%, 80% and 95% percentiles of the Monte Carlo simulation estimates (which we loosely call confidence bands), together with the median, obtained, respectively, with the cubic splines and the RBBF methods, when $T = 200$ (Figures A.7 and A.8 show the same results when $T = 500$). The results discussed above are confirmed by these Figures. Both methods are able to pick up the true time-variation of the correlation parameter, and their estimation performance improves with a larger sample size. The RBBF is therefore robust to misspecifications of the dynamic structure of ρ_t since none of the true correlations displayed in the Figures is a random walk. The confidence bands for the cubic splines are narrower, except towards the end of the sample, and less volatile than their RBBF's counterparts, but the fast sine DGP of ρ_t is estimated almost as constant by the cubic splines method, contrary to the RBBF. Notice also that the RBBF is slightly delayed in time with respect to the true time variation in ρ_t, which is to be expected from filters, since they are only based on past information, contrary to the time-constant estimation and the cubic splines (a particle smoother would not show this delay). Although the indirect inference method estimates the static parameters based on the entire sample, the RBBF can therefore be considered a real-time estimator. For this reason the time-constant and cubic splines methods are

rewarded too much by the simulations study, with respect to the RBBF. A real-time comparison of the methods would tend to favour more the latter. In a simulation study, van den Brakel and Krieg (2016) showed that with a time constant correlation between survey and claimant counts data, it takes more than a year before the maximum likelihood estimate for the correlation picks up a change in the relation between the two series. However, for computational purposes, we only perform such a comparison in the empirical application of Section 5, since it is also of interest for the production of official statistics. The scope of the simulation study is just to understand to which extent the employed methods appropriately estimate, on average, the (time-varying) parameters.

Figures A.9-A.12 report the absolute MSE and squared bias of $\hat{\rho}_t$, over time, for all estimations methods (including the method that estimates the correlation as static). These pictures reveal an information that was hidden in Tables 4.1 and A.1, but already partly discovered from Figures 4.2, 4.3, A.7 and A.8: a better performance of the RBBF over the cubic splines, in terms of MSE, at the end of the sample, when $T = 200$. This is due to the large uncertainty that affects the cubic splines at the boundaries of the sample (we cannot conclude the same for the start of the sample because the performance of the RBBF there very much depends on the initial values for γ_t). In terms of squared bias and when $T = 500$, the two methods tend instead to perform similarly while approaching the end of the sample. What also appears from these Figures is that, when there are structural changes (i.e., when the true DGP of ρ_t is either a step or a ramp function) the RBBF is much worse in estimating the correlation *at* the change point in time, with respect to the other methods, due to its delayed behaviour. However, a real-time comparison would, also in this case, reward less the methods based on maximum likelihood.

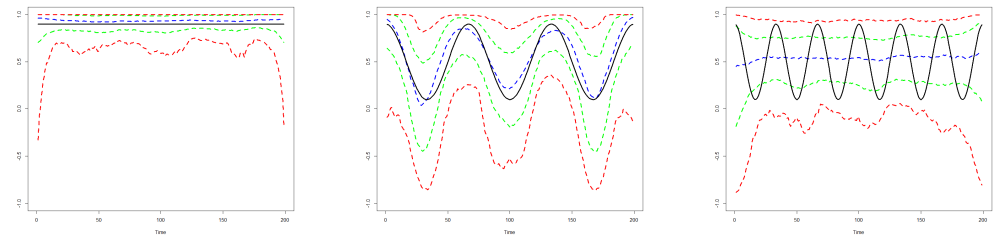

(a) Constant (b) Sine (c) Fast sine

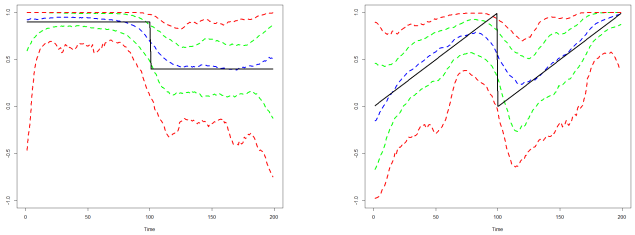

(d) Step (e) Ramp

Figure 4.2 True process of ρ_t (black) together with the 95% (red), 80% (green) confidence bands, and the median (blue) of the simulation estimates for the cubic splines estimator of ρ_t. $T = 200$, $S = 3$, $M = 5000$, $n_{\text{sim}} = 500$.

Finally, the relative MSE and squared bias of $\hat{L}_{y,t}$ in Table 4.1 are generally around 1 for all DGPs of ρ_t and for both estimation methods, also when the sample size is large. This result indicates that estimating the correlation as time-varying, also when appropriate, instead of time-constant, does not have an impact on the estimation accuracy of the

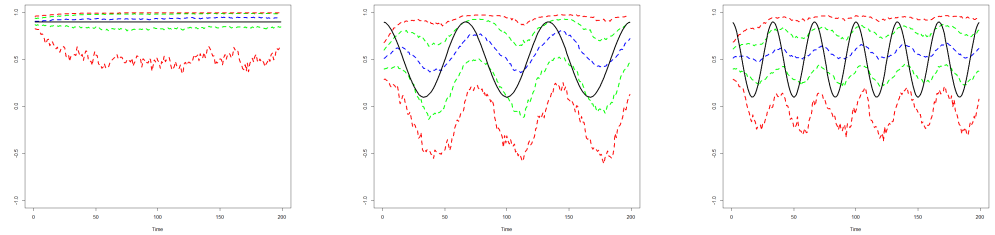

(a) Constant (b) Sine (c) Fast sine

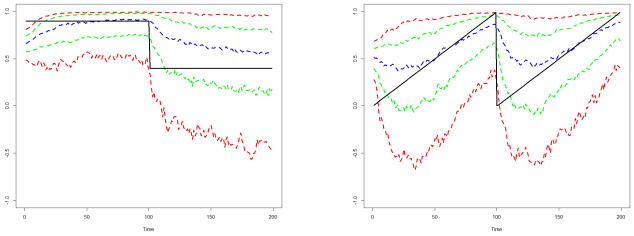

(d) Step (e) Ramp

Figure 4.3 True process of ρ_t (black) together with the 95% (red), 80% (green) confidence bands, and the median (blue) of the simulation estimates for the Rao-Blackwellised bootstrap filter estimator of ρ_t. $T = 200$, $S = 3$, $M = 5000$, $n_{\text{sim}} = 500$.

state variable of interest, probably due to the Kalman filter's high accuracy in estimating unobserved components, irrespectively of the parameters' estimates. Nonetheless, results from Section 5 suggest that in a real-time estimation these conclusions would be different. Figures A.13-A.16 show the absolute MSE and the squared bias of $\hat{L}_{y,t}$ over time, for all estimation methods. Except for a slightly worse performance, in terms of MSE, of the RBBF when $T = 200$, and a slightly better one of the cubic splines when $T = 500$, it is almost impossible to tell the difference, among methods, in the estimation accuracy of $L_{y,t}$. What appears evident from these Figures, however, is how the magnitude of the MSE tends to follow the time-varying pattern of ρ_t (for its deterministic DGPs): the MSE is lower when the magnitude of the correlation is larger, as the auxiliary series brings in this case more information about the state variable of interest.

In conclusion, the Monte Carlo simulation study shows that our proposed indirect inference method is able to correctly estimate the time-invariant parameters of the nonlinear model. Only the finite-sample distribution of the indirect inference estimator of σ_γ is not symmetrical, suggesting that it is not normal either. Nevertheless, since we do not carry out any inference on this parameter, we do not need normality of the estimator to hold[8]. Both the cubic splines and the RBBF approaches are suited to estimate a time-varying state correlation. The former method, on average, always beats the latter, in terms of estimation accuracy of ρ_t, due to the strong volatility that affects the RBBF, except when it comes to estimate correlations that change rapidly over time. Moreover, with small sample sizes, the RBBF yields more precise estimates for ρ_t towards the end of the sample, which is relevant when the focus is on exploring how the relationship between the observed series has evolved in recent times. The estimation accuracy of all methods (indirect inference, cubic splines and RBBF) improves with the

[8] Notice that providing theoretical properties for the indirect inference estimators is beyond the scope of this paper. However, we point out that the knowledge of such asymptotic distribution would allow to test for time-constancy in the correlation parameter, by testing whether $\sigma_\gamma = 0$.

sample size. Appropriately estimating the time-varying correlation as such, instead of as time-constant, does not affect the estimation accuracy of state variables of interest. The RBBF is a real-time estimator of the correlation (i.e., it only exploits past information), whereas the time-constant and cubic splines methods estimate this parameter based on the entire sample. The simulation results here obtained therefore tend to reward too much the latter approaches. In real-time, the RBBF would yield an even better performance with respect to the other two methods. Such a real-time comparison is not explored in the Monte Carlo simulation study, but is investigated in the upcoming Section.

5 Empirical application to the extended Dutch labour force model

In this Section we perform the in-sample estimation of the Dutch labour force model extended with the univariate series of claimant counts, described in Section 2. We model the time-varying correlation with our proposed methodology based on indirect inference and Rao-Blackwellised bootstrap filtering. As done in the Monte Carlo simulation study, we compare the results so obtained to estimating the correlation parameter as time constant, and with the cubic splines method only. We also investigate the sensitivity of our results to the location of the cubic splines' knots. Specifically, we first consider the case where the (five, as suggested by the BIC) knots correspond to the quartiles of the sample. Then, we examine the case when February 2015 is one of the knots (since we know that a potential change in the correlation happened on this date), and the remaining (four) knots are chosen accordingly in order to keep an approximately equal distance between each pair of knots. Finally, we compare the performance of the methods when the estimation of the model is conducted in real-time, and not only on the entire sample. We use monthly data from January 2004 until March 2020 ($T = 195$) for both the GREG estimates and the claimant counts, $S = 5$ simulations for the indirect inference method, and $M = 5000$ particles for the RBBF.

Figure 5.1 displays the estimated correlation, ρ_t, and its unbounded counterpart, γ_t, with all three methods, when the knots are located at the quartiles of the sample. The time-constant estimate for ρ_t is positive and very large, but it hides the decrease of the correlation parameter that occurred in the middle of the sample. Indeed, both the cubic splines and the RBBF estimates of ρ_t indicate that the two types of observed series started deviating from each other in 2010, that is, around two years after the financial crisis of 2008. Recession periods can induce long-term unemployment, and in the Netherlands unemployment benefits cannot be claimed for more than three years and two months, despite being unemployed or not, at the end of this period. However, not everyone is entitled to receive benefits for the maximum amount of time. The long-term unemployment caused by the economic crisis of 2008 is therefore not entirely picked up by the claimant counts series, which hence starts deviating from the GREG estimates around two years after the burst of the crisis. The magnitude of the correlation increased again in 2013, and stabilized around its ante-crisis levels from 2017 until the most recent times. Remember from the results of the Monte Carlo simulation study,

that it is the RBBF estimate that provides the most reliable information on the behaviour of the parameter towards the end of the sample, which is indeed when the RBBF and the cubic splines estimates deviate the most from each other. We also notice how the RBBF, but not the cubic splines, captures a drop in the correlation after the legislative change of February 2015. New legislations often apply to new claims of unemployment benefits, which explains why the correlation does not drop immediately in February 2015, but shorty after. This decrease is, however, not as deep and prolonged as the one caused by the financial crisis of 2008.

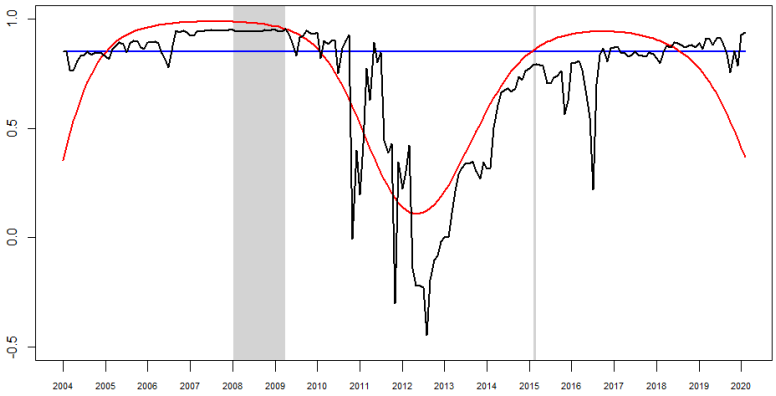

(a) $\hat{\rho}_t$

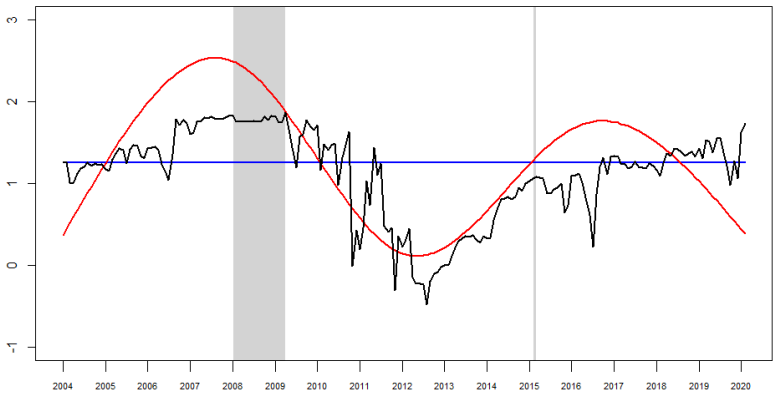

(b) $\hat{\gamma}_t$

Figure 5.1 Time constant (blue), cubic splines (red) and RBBF (black) estimates of ρ_t and γ_t, from the Dutch labour force model extended with the auxiliary series of claimant counts (described in Section 2). Monthly data from January 2004 until March 2020 ($T = 195$), $S = 5$, $M = 5000$. The knots for the cubic splines approach correspond to the quartiles of the sample. The first shaded area represent the recession period due to the financial crisis of 2008, whereas the second one refers to the legislative change of February 2015.

Noteworthy, Figure 5.1 further shows how the RBBF method yields a much more volatile estimate for ρ_t, than the cubic splines, which partly reflects estimation error. We already concluded from the simulation study of Section 4, that the volatility of the RBBF estimator represents its Achilles' heel. Although we do not implement them in the paper, we here give two suggestions that could potentially correct for this problem. First,

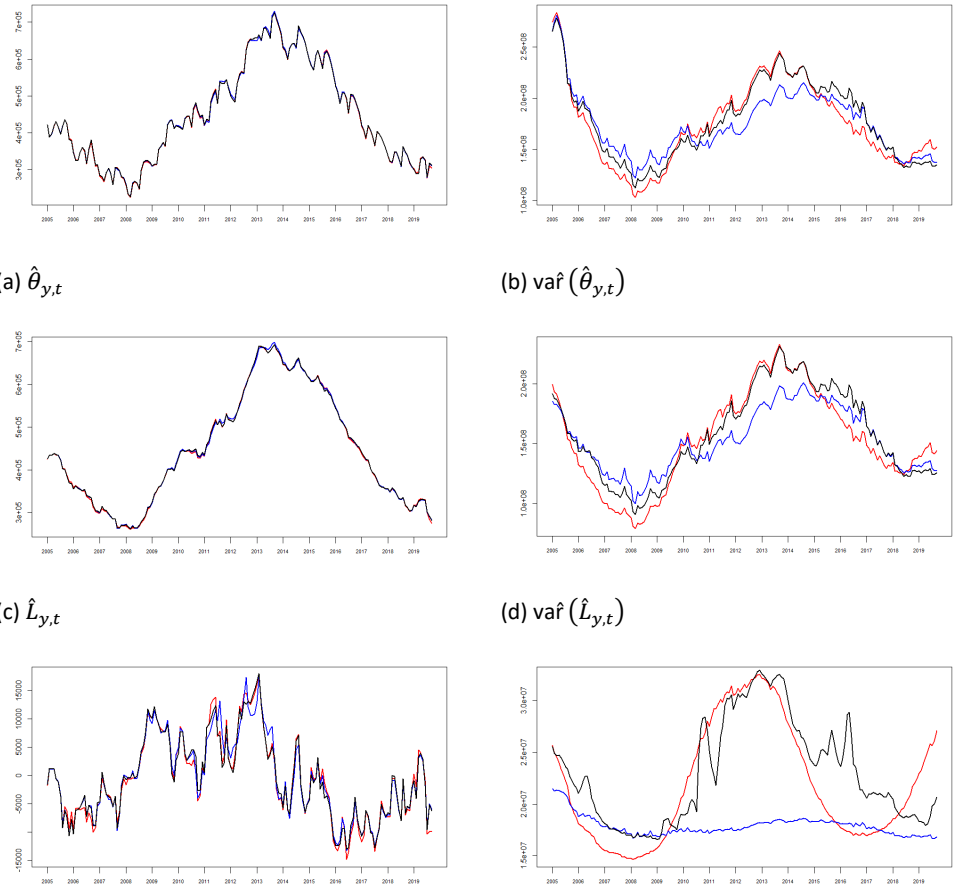

(a) $\hat{\theta}_{y,t}$ (b) var̂ $(\hat{\theta}_{y,t})$

(c) $\hat{L}_{y,t}$ (d) var̂ $(\hat{L}_{y,t})$

(e) $\hat{R}_{y,t}$ (f) var̂ $(\hat{R}_{y,t})$

Figure 5.2 Kalman filter estimates (left panels) and respective estimated variances (right panels) of the state variables of interest $\theta_{y,t}$, $L_{y,t}$ and $R_{y,t}$, in the Dutch labour force model extended with the auxiliary series of claimant counts (described in Section 2). The results are obtained when the correlation parameter is estimated as constant (blue), with the cubic splines method (red), and with the RBBF (black). Monthly data from January 2004 until March 2020 ($T = 195$), $S = 5$, $M = 5000$. The knots for the cubic splines approach correspond to the quartiles of the sample. The first d months are not displayed because of the Kalman's filter diffuse initialisation.

a bootstrap smoother (instead of a filter) should yield, as its name gives away, a smoother estimate for ρ_t. Second, we explain in Section 3.2 how we modify the resampling step of the RBBF's algorithm, in order to keep particles that yield slightly larger likelihood values. We mentioned that without this modification, the filtered estimate for the correlation would almost be constant over time. We arbitrarily decided to take the $p_t = \ln\left(\frac{\sqrt{M-1}}{CV_t}\right)$ power of the normalised weights in order to achieve our goal. However, this function may increase the differences among weights too much and therefore make the RBBF too volatile. Many other functions of the normalised weights can be applied instead and potentially diminish the volatility of the filter.

Figure B.1 compares the cubic splines and RBBF estimates for ρ_t that have been discussed above, with the ones obtained for the second choice of knots' location (which uses February 2015 as one of the knots). The estimates are not sensitive to the location of the knots, if not for a slightly larger volatility of the cubic splines estimate with the second choice of knots' location, which is inherited also by the RBBF estimate.

		Knots at quartiles		Knots include February 2015	
	Maximum likelihood		Indirect inference	Maximum likelihood	Indirect inference
	Constant	Cubic splines		Cubic splines	
$\hat{\sigma}_{R,y}$	2719.916	3011.516	2996.161	2953.373	2971.015
$\hat{\sigma}_{\omega,y}$	0.016	0.028	0.02	0.044	0.044
$\hat{\sigma}_{\lambda}$	3778.169	3739.127	3831.573	3695.226	3690.149
$\hat{\sigma}_{v_1}$	1.335	1.322	1.261	1.328	1.331
$\hat{\sigma}_{v_2}$	1.309	1.304	1.260	1.3	1.272
$\hat{\sigma}_{v_3}$	1.199	1.192	1.106	1.186	1.176
$\hat{\sigma}_{v_4}$	1.234	1.234	1.173	1.235	1.229
$\hat{\sigma}_{v_5}$	1.219	1.214	1.179	1.22	1.22
$\hat{\delta}$	0.378	0.38	0.327	0.378	0.375
$\hat{\sigma}_{R,CC}$	3422.074	3453.365	3371.296	3485.617	3282.554
$\hat{\sigma}_{\omega,CC}$	0.019	0.021	0.02	0.01	0.01
$\hat{\sigma}_{\varepsilon,CC}$	1499.447	1481.391	1479.833	1462.325	1466.448
$\hat{\rho}$	0.851				
$\hat{\phi}_1$		0.367		-0.629	
$\hat{\phi}_2$		2.484		2.39	
$\hat{\phi}_3$		0.127		-0.098	
$\hat{\phi}_4$		1.697		1.386	
$\hat{\phi}_5$		0.333		0.269	
$\hat{\sigma}_{\gamma}$			0.081		0.127
Log-likelihood	-12549.42	-12546.34	-12476.98	-12547.15	-12475.59

Table 5.1 The columns named "Maximum likelihood" report the maximum likelihood estimates of the static parameters of the Dutch labour force model extended with the auxiliary series of claimant counts (described in Section 2), when the correlation parameter is estimated as time constant and with the cubic splines method. The remaining columns show the indirect inference estimates of the static parameters (including σ_γ). "Knots at quartiles" means that the knots for the cubic splines approach correspond to the quartiles of the sample; they are otherwise approximately equally distant by fixing February 2015 as knot. The log-likelihood values are obtained by evaluating the Kalman filter recursions (3.4) at the corresponding estimates for ρ_t and the static parameters.

Table 5.1 reports the estimates of the static parameters for each considered model. The indirect inference estimate for σ_γ is indeed larger when February 2015 is part of the knots. The table also displays the log-likelihood values that are obtained by evaluating the Kalman filter recursions (3.4), and subsequent likelihood function (3.2), at the corresponding estimates for ρ_t and the static parameters. Although we cannot perform a formal test on these log-likelihood values, because we are comparing non-nested models, we can still conclude that the estimation based on indirect inference and RBBF always yields a better fit of the data.

We employ the BFGS and a conjugate gradient optimisation algorithm when we estimate the static parameters, respectively, by maximum likelihood and by indirect inference. The complexity of the Dutch labour force model hampers its estimation by indirect inference with the BFGS algorithm. When estimating the static parameters by maximum likelihood, we use their estimates from the labour force model obtained in van den Brakel and Krieg (2015), as initial values. The initial values of the static parameters in the indirect inference estimation are instead equal to the corresponding maximum likelihood estimates obtained with the cubic splines model.

Figure 5.2 plots the Kalman filter estimates and respective estimated variances (i.e., the corresponding elements of $a_{t|t}$ and $P_{t|t}$ in the Kalman filter recursions (3.4)) of the state

variables of interest $\theta_{y,t}$, $L_{y,t}$ and $R_{y,t}$, in the extended Dutch labour force model. The results refer to the setting where the knots correspond to the quartiles of the sample. The point estimates of the state variables are slightly sensitive to the estimation method of ρ_t, especially in the middle of the sample where the difference between time-constant and time-varying estimates for ρ_t is largest. The estimated variances are much more dependent on the magnitude of the correlation's estimates: they are larger when the estimated correlation shrinks, i.e., when the claimant counts bring less information about the Dutch unemployment. This is especially evident for $R_{y,t}$, than the other two state variables, since the slopes of the series' trends are directly related to each other via ρ_t. The estimated variances, when the correlation is estimated as time-constant, are generally very low (given the large value of the correlation's estimate). This may suggest that treating ρ_t as time-constant improves the estimation accuracy of state variables of interest. However, these variances are, in this case, wrongly estimated if the true process for ρ_t is time-varying. The variance estimates obtained with the cubic splines and the RBBF methods, although larger in the middle of the sample, are therefore more realistic as they reflect the economic uncertainty of that period. We again notice a better performance of the RBBF, with respect to the cubic splines method, in the estimation accuracy of the state variables towards the end of the sample. Notice that these estimated variances do not also reflect the additional uncertainty of using estimates for ρ_t and the static parameters.

Finally, Figure B.2 compares the estimated correlation, when this is treated as static, to the same estimates obtained with shorter samples. Namely, we use five sub-samples that include observed monthly data form January 2004 up until and including years 2010-2014 (notice that extending the sample with one additional year corresponds to including twelve additional monthly observations). The time-constant correlation model shows a delay of around four years in picking up the deviation between the survey-based data and the claimant counts. This result further stresses the need for an approach that is able to capture the time-variation of the correlation in a more timely manner, which is achieved by the RBBF rather than the cubic splines method. We therefore conduct a real-time exercise where we estimate the state variables of interest for the sub-samples mentioned above, while estimating the correlation as static and with the RBBF[9)]. We compare these results to the ones obtained with the Dutch labour force model that does not include any auxiliary series[10)]. Figures B.3-B.5 and B.6-B.8 respectively show the Kalman filter estimates of the three state variables of interest, and their estimated variances, obtained for all models and sub-samples (as well as for the entire sample, which ends in March 2020)[11)]. We notice that, until the end of 2010 and from 2014, the RBBF and the time-constant correlation models both yield close estimates to the ones obtained with the model that does not include auxiliary series. Between these years,

9) We do not also perform the real-time analysis with the cubic splines estimation method for the correlation, since the large uncertainty that affects cubic splines at the end of the sample makes this method unsuited for real-time estimation.

10) Whenever we add an additional year of observations, we re-estimate the static parameters, by maximum likelihood, of the time-constant correlation model and the one without auxiliary series. The static parameters of the model that employs the RBBF are instead, for computational purposes, always kept equal to the ones obtained by indirect inference for the entire sample (and with knots corresponding to the quartiles of the sample).

11) Notice that in these Figures the (variance) estimate for the last point in time is not reported when the RBBF is employed, because the algorithm used for the RBBF does not provide such estimate. This issue is discussed in Section 3.2.

however, the latter estimates are much closer to the ones provided by the model which employs the RBBF, rather that the time-constant correlation one. This deviation is due to the incapability of the static correlation estimation method to quickly detect and capture the change in the correlation parameter, contrary to the RBBF. We here use the model without auxiliary series as benchmark, not because we treat is as the true one, but because too large deviations between the states' estimates that it yields and the ones obtained with other models, are an indication that some time-varying characteristics are not being taken into account. The variance estimates for $\theta_{y,t}$ and $L_{y,t}$ are always larger, except in the middle of the sample, for the model that does not include auxiliary series as it does not exploit any additional information. The estimation of $R_{y,t}$ is instead affected by a much stronger uncertainty, represented by larger variance estimates, when the RBBF is employed for the estimation of the correlation.

6 Conclusions

This paper proposes a new methodology to estimate nonlinear state space models, where the nonlinearity arises from a stochastic state correlation. The static parameters are estimated with an indirect inference approach, which employs a cubic splines specification for the time-varying correlation as auxiliary model. The stochastic correlation and remaining state variables are instead estimated with the Rao-Blackwellised bootstrap filter (RBBF). We perform a Monte Carlo simulation study and an empirical application to Dutch unemployment estimation, in order to evaluate the performance of our methodology. In the empirical analysis the correlation represents the relationship between survey-based data about the unemployed labour force, and the series of claimant counts. We compare our method to estimating the time-varying correlation by means of cubic splines only, and as time-constant.

The Monte Carlo simulation study shows that both the cubic splines and the RBBF methods are able to capture the true time-varying pattern of the correlation. This parameter is, on average, more accurately estimated by the former approach. The latter is affected by a strong volatility that tends to deteriorate its performance. This issue also arises from the results of the empirical application. In Section 5 we therefore mention two possible solutions that could correct for this problem. Nevertheless, the RBBF beats the cubic splines method in estimating correlations that change rapidly over time, and in yielding more accurate estimates for the correlation towards the end of the sample, especially when sample sizes are small. These latter results already highlight the usefulness of the RBBF in case of real-time estimation.

Both the cubic splines and the RBBF estimators of the correlation are more volatile that the time-constant one, due to their time-varying nature. Hence, in small samples they beat the latter method in terms of squared bias but not in terms of mean squared error (which also captures the volatility of an estimator).

The indirect inference estimators appropriately estimate the static parameters, as their finite-sample distributions are centered around them. Although these distributions are not all symmetrical when sample sizes are small, their shape improves with a larger

sample size. So does the performance of the cubic splines and the RBBF estimators, also with respect to estimating the correlation as static.

The point estimates of state variables of interest, when the estimation is not conducted in real-time, do not depend on the method that is employed for the estimation of the time-varying correlation, as much as their estimated variances do. The larger the magnitude of the estimated correlation, the lower the variance estimates of the state variables. In other words, the more information the auxiliary series brings about the variables of interest, the more accurate the estimates for the latter are. Results from the empirical application suggest that the states' estimates can instead be rather different when obtained in real time, depending on the method used for the estimation of the correlation. Specifically, the RBBF promptly detects changes in the correlation parameter, thus yielding more reliable states' estimates. The static estimation of the correlation parameter, on the other hand, is affected by a strong delay in tackling such changes, which is reflected in unrealistic real-time estimates of the state variables. Moreover, the cubic splines method is not suited for real-time estimation because of its uncertainty in estimating the correlation towards the end of the sample. Real-time estimation of variables is important in the context of official statistics, and finding a method that is reliable for this purpose, such as the RBBF, is an important result.

Empirically, the cubic splines and RBBF agree in estimating a strong and positive correlation in the first and last years of the sample. They capture a deviation between the two types of observed series in the middle of the sample, which is caused by the financial crisis of 2008. The long-term unemployment induced by this recession period can indeed not be completely picked up by the claimant counts. Moreover, only the RBBF manages to tackle an additional drop in the correlation parameter after the implementation of a legislative change that affected the claimant counts series in 2015. This decrease is, however, less protracted and of smaller magnitude than the one triggered by the financial crisis.

In this paper we employ only one auxiliary series in the state space model, and hence deal with estimating only one time-varying correlation parameter. Our proposed method can theoretically be extended to the case where more than one auxiliary series are included in the model, and therefore several correlation parameters need to be estimated. However, the indirect inference and the RBBF are both simulation-based methods and are, as such, computationally rather expensive. Hence, the model should not be too complex in order to guarantee a successful performance of our proposed method.

References

Antolin-Diaz, J., Drechsel, T., and Petrella, I. (2017). Tracking the Slowdown in Long-run GDP Growth. *Review of Economics and Statistics* 99 (2), 343–356.

Bailar, B. (1975). The Effects of Rotation Group Bias on Estimates from Panel Surveys. *Journal of the American Statistical Association* 70 (349), 23–30.

Bollineni-Balabay, O., van den Brakel, J., and Palm, F. (2017). State Space Time Series Modelling of the Dutch Labour Force Survey: Model Selection and Mean Squared Errors Estimation. *Survey Methodology* 43 (1), 41–67.

Chen, R. and Liu, J. S. (2000). Mixture Kalman Filters. *Journal of the Royal Statistical Society: Series B (Statistical Methodology)* 62 (3), 493–508.

Chen, R., Liu, J. S., and Logvinenko, T. (2001). A Theoretical Framework for Sequential Importance Sampling with Resampling. In *Sequential Monte Carlo Methods in Practice. Statistics for Engineering and Information Science.*, Chapter 11, pp. 225–246. Springer, New York.

Creal, D. (2012). A Survey of Sequential Monte Carlo Methods for Economics and Finance. *Econometric Reviews* 31 (3), 245–296.

Creal, D., Koopman, S. J., and Lucas, A. (2011). A Dynamic Multivariate Heavy-Tailed Model for Time-Varying Volatilities and Correlations. *Journal of Business & Economic Statistics* 29 (4), 552–563.

Creal, D., Koopman, S. J., and Lucas, A. (2013). Generalized Autoregressive Score Models with Applications. *Journal of Applied Econometrics* 28 (5), 777–795.

Delle Monache, D., Petrella, I., and Venditti, F. (2016). Adaptive State Space Models with Applications to the Business Cycle and Financial Stress.

Durbin, J. and Koopman, S. J. (2012). *Time Series Analysis by State Space Methods* (Second ed.). Oxford Statistical Science Series. OUP Oxford.

Gagliardini, P., Ghysels, E., and Rubin, M. (2017). Indirect Inference Estimation of Mixed Frequency Stochastic Volatility State Space Models Using MIDAS Regressions and ARCH Models. *Journal of Financial Econometrics* 15 (4), 509–560.

Gallant, A. R. and Tauchen, G. (1998). Reprojecting Partially Observed Systems with Application to Interest Rate Diffusions. *Journal of the American Statistical Association* 93 (441), 10–24.

Gordon, N. J., Salmond, D. J., and Smith, A. F. M. (1993). A Novel Approach to Nonlinear and Non-Gaussian Bayesian State Estimation. *IEE Proceedings. Part F: Radar and Sonar Navigation* 140 (2), 107–113.

Gourieroux, C., Monfort, A., and Renault, E. (1993). Indirect Inference. *Journal of Applied Econometrics* 8, 85–118.

Hansen, B. E. (2019). *Econometrics* (Jan 2019 ed.). University of Wisconsin, Department of Economics.

Harvey, A. and Chung, C.-H. (2000). Estimating the Underlying Change in Unemployment in the UK. *Journal of the Royal Statistical Society: Series A (Statistics in Society)* 163 (3), 303–309.

Harvey, A. C. (1989). *Forecasting, Structural Time Series Models and the Kalman Filter*. Cambridge University Press.

Harvey, A. C. (2013). *Dynamic Models for Volatility and Heavy Tails: with Applications to Financial and Economic Time Series*. Economic Series Monograph. Cambridge University Press.

Hastie, T., Tibshirani, R., and Friedman, J. (2009). *The Elements of Statistical Learning*. Springer Series in Statistics. New York, NY, US: Springer New York Inc.

Jungbacker, B. and Koopman, S. J. (2007). Monte Carlo Estimation for Nonlinear Non-Gaussian State Space Models. *Biometrika* 94 (4), 827–839.

Kitagawa, G. (1996). Monte Carlo Filter and Smoother for Non-Gaussian Nonlinear State Space Models. *Journal of Computational and Graphical Statistics* 5 (1), 1–25.

Koopman, S. J., Lee, K. M., and Wong, S. Y. (2006). Trend-Cycle Decomposition Models with Smooth-Transition Paramteres: Evidence from U.S. Economic Time Series. In *Nonlinear Time Series Analysis of Business Cycles*, Contributions to Economic Analysis, Chapter 8, pp. 199–219. Emerald Group Publishing Limited.

Koopman, S. J., Lit, R., and Nguyen, T. M. (2018). Modified Efficient Importance Sampling for Partially Non-Gaussian State Space Models. *Statistica Neerlandica* 73 (1), 44–62.

Koopman, S. J., Lucas, A., and Scharth, M. (2015). Numerically Accelerated Importance Sampling for Nonlinear Non-Gaussian State-Space Models. *Journal of Business and Economic Statistics* 33 (1), 114–127.

Li, T., Bolić, M., and Djurć, P. M. (2015). Resampling Methods for Particle Filtering: Classification, Implementation, and Strategies. *IEEE Signal Processing Magazine* 32 (3), 70 – 86.

Liu, J. S. and Chen, R. (1998). Sequential Monte Carlo Methods for Dynamic Systems. *Journal of the American Statistical Association* 93 (443), 1032–1044.

Monfardini, C. (1998). Estimating Stochastic Volatility Models through Indirect Inference. *The Econometrics Journal* 1 (1), C113–C128.

Pfeffermann, D. (1991). Estimation and Seasonal Adjustment of Population Means Using Data from Repeated Surveys. *Journal of Business and Economic Statistics* 9 (2), 163–175.

Pfeffermann, D., Feder, M., and Signorelli, D. (1998). Estimation of Autocorrelations of Survey Errors with Application to Trend Estimation in Small Areas. *Journal of Business & Economic Statistics* 16 (3), 339–348.

Poirier, D. J. (1973). Piecewise Regression Using Cubic Splines. *Journal of the American Statistical Association* 68 (343), 515–524.

Proietti, T. and Hillebrand, E. (2017). Seasonal Changes in Central England Temperatures. *Journal of the Royal Statistical Society: Series A (Statistics in Society)* 180 (3), 769–791.

Rao, J. N. K. and Molina, I. (2015). *Small Area Estimation* (2 ed.). Wiley Series in Survey Methodology. John Wiley & Sons, Inc.

Särndal, C.-E., Swensson, B., and Wretman, J. (1992). *Model Assisted Survey Sampling*. New York, NY, US: Springer-Verlag Publishing.

Schiavoni, C., Palm, F., Smeekes, S., and van den Brakel, J. (2021). A Dynamic Factor Model Approach to Incorporate Big Data in State Space Models for Official Statistics. *Journal of the Royal Statistical Society: Series A (Statistics in Society)* 184 (1), 324–353.

Shephard, N. G. and Harvey, A. C. (1990). On the Probability of Estimating a Deterministic Component in the Local Level Model. *Journal of Time Series Analysis* 11 (4), 339–347.

Smith, P. L. (2008). Splines As a Useful and Convenient Statistical Tool. *The American Statistician* 33 (2), 57–62.

Stock, J. H. and Watson, M. W. (1998). Median Unbiased Estimation of Coefficient Variance in a Time-varying Parameter Model. *Journal of the American Statistical Association* 93 (441), 349–358.

Stock, J. H. and Watson, M. W. (2007). Why Has U.S. Inflation Become Harder to Forecast? *Journal of Money, Credit and Banking* 39 (1), 3–33.

van den Brakel, J. and Krieg, S. (2009). Estimation of the Monthly Unemployment Rate Through Structural Time Series Modelling in a Rotating Panel Design. *Survey Methodology* 35 (2), 177–190.

van den Brakel, J. A. and Krieg, S. (2015). Dealing with Small Sample Sizes, Rotation Group Bias and Discontinuities in a Rotating Panel Design. *Survey Methodology* 41 (2), 267–296.

van den Brakel, J. A. and Krieg, S. (2016). Small Area Estimation with State Space Common Factor Models for Rotating Panels. *Journal of the Royal Statistical Society: Series A (Statistics in Society)* 179 (3), 763–791.

Appendix

A Additional results from the Monte Carlo simulation study

	$T = 200$						$T = 500$					
	0.9	Sine	Fast sine	Step	Ramp	Random walk	0.9	Sine	Fast sine	Step	Ramp	Random walk
						Cubic splines						
MSE$(\hat{\rho}_t)$	0.041	0.159	0.206	0.092	0.130	0.124	0.005	0.053	0.116	0.030	0.057	0.051
bias$^2(\hat{\rho}_t)$	0.001	0.007	0.081	0.004	0.015	1.4e-04	3.9e-05	0.010	0.080	0.004	0.014	1.1e-04
MSE$(\hat{L}_{y,t})$	0.508	0.597	0.608	0.565	0.592	0.585	0.500	0.584	0.595	0.555	0.583	0.586
bias$^2(\hat{L}_{y,t})$	0.001	0.001	0.001	0.001	0.001	0.001	0.001	0.001	0.001	0.001	0.001	0.001
						Rao-Blackwellised bootstrap filter						
MSE$(\hat{\rho}_t)$	0.045	0.172	0.161	0.113	0.172	0.171	0.009	0.129	0.103	0.070	0.129	0.095
bias$^2(\hat{\rho}_t)$	0.001	0.050	0.067	0.019	0.037	3.4e-04	1.3e-04	0.030	0.070	0.014	0.028	2.2e-04
MSE$(\hat{L}_{y,t})$	0.946	0.669	0.649	0.746	0.737	0.700	0.527	0.638	0.600	0.602	0.622	0.609
bias$^2(\hat{L}_{y,t})$	0.002	0.002	0.001	0.002	0.002	0.002	0.001	0.001	0.001	0.001	0.001	0.001
						Ideal Rao-Blackwellised bootstrap filter						
MSE$(\hat{\rho}_t)$						0.159						0.099
bias$^2(\hat{\rho}_t)$						3.1e-04						1.3e-04
MSE$(\hat{L}_{y,t})$						0.594						0.596
bias$^2(\hat{L}_{y,t})$						0.001						0.001
						Constant						
MSE$(\hat{\rho}_t)$	0.002	0.094	0.094	0.072	0.097	0.135	0.001	0.085	0.085	0.067	0.089	0.089
bias$^2(\hat{\rho}_t)$	1.7e-05	0.080	0.080	0.063	0.083	2.9e-04	1.4e-06	0.080	0.080	0.062	0.083	0.083
MSE$(\hat{L}_{y,t})$	0.501	0.596	0.599	0.575	0.597	0.596	0.498	0.594	0.593	0.572	0.572	0.594
bias$^2(\hat{L}_{y,t})$	0.001	0.001	0.001	0.001	0.001	0.001	0.001	0.001	0.001	0.001	0.001	0.001

Table A.1 Mean squared error and squared bias for the cubic splines, the Rao-Blackwellised bootstrap filter and the constant estimators of ρ_t, and the Kalman filter estimator of $L_{y,t}$. The second row lists the DGPs for ρ_t. "Ideal Rao-Blackwellised bootstrap filte" indicates that the static parameter vector τ is treated as known. $S = 3$, $M = 5000$, $n_{\text{sim}} = 500$.

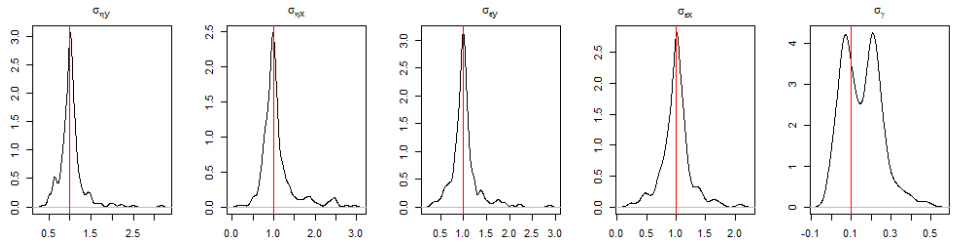

(a) $T = 200$

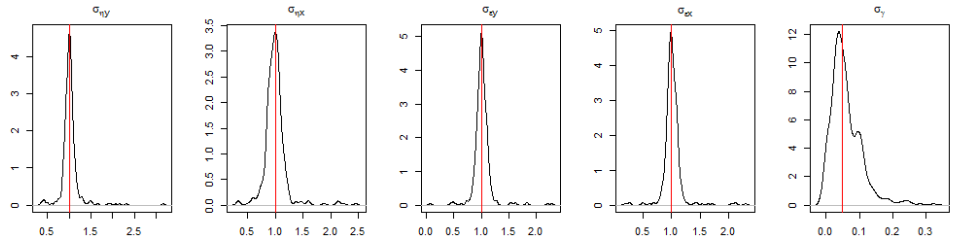

(b) $T = 500$

Figure A.1 Distribution of the indirect inference estimators of the static parameters of the nonlinear model, $\tau = \left(\sigma_{\eta,y}, \sigma_{\eta,x}, \sigma_{\varepsilon,y}, \sigma_{\varepsilon,x}, \sigma_{\gamma}\right)'$, based on the Monte Carlo replicates, when the DGP of ρ_t is a random walk and the BFGS algorithm is not started at the true values; $S = 3$, $n_{\text{sim}} = 500$. The red lines represent the true values of the parameters.

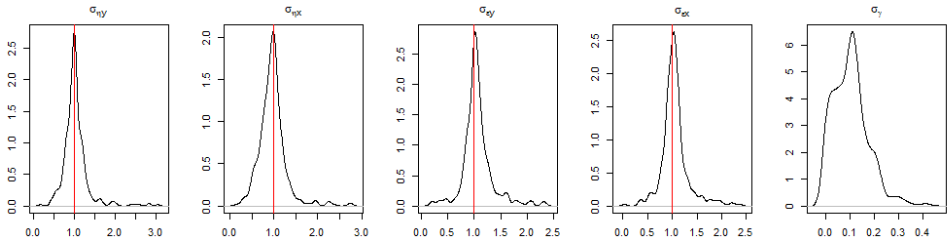

(a) $T = 200$

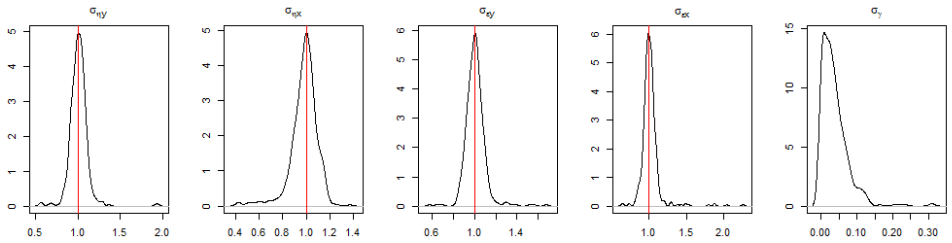

(b) $T = 500$

Figure A.2 Distribution of the indirect inference estimators of the static parameters of the nonlinear model, $\tau = \left(\sigma_{\eta,y}, \sigma_{\eta,x}, \sigma_{\varepsilon,y}, \sigma_{\varepsilon,x}, \sigma_{\gamma}\right)'$, based on the Monte Carlo replicates, when the DGP of ρ_t is constant and equal to 0.9; $S = 3$, $n_{\text{sim}} = 500$. The red lines represent the true values of the parameters.

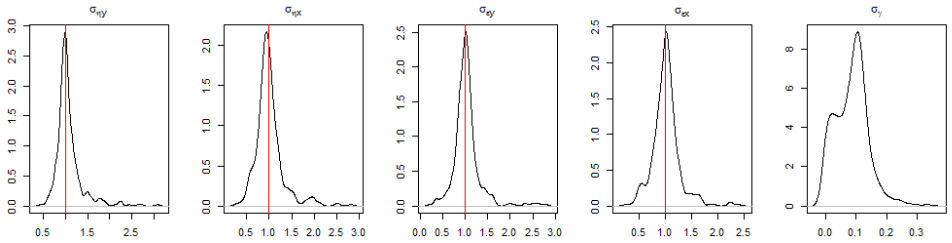

(a) $T = 200$

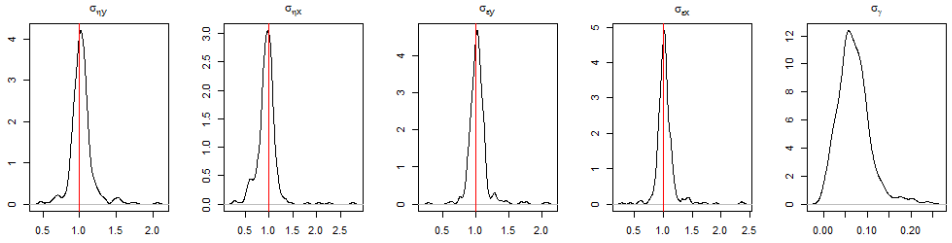

(b) $T = 500$

Figure A.3 Distribution of the indirect inference estimators of the static parameters of the nonlinear model, $\tau = \left(\sigma_{\eta,y}, \sigma_{\eta,x}, \sigma_{\varepsilon,y}, \sigma_{\varepsilon,x}, \sigma_{\gamma}\right)'$, based on the Monte Carlo replicates, when the DGP of ρ_t is a sine function; $S = 3$, $n_{\text{sim}} = 500$. The red lines represent the true values of the parameters.

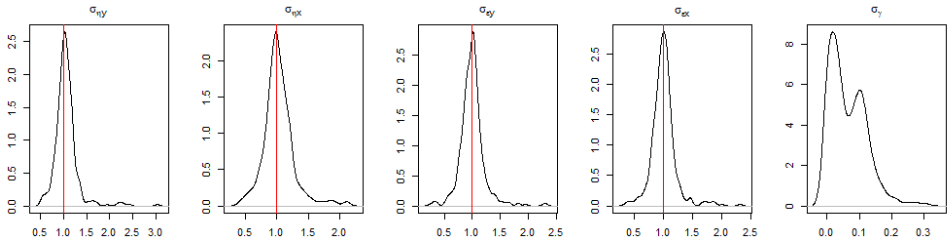

(a) $T = 200$

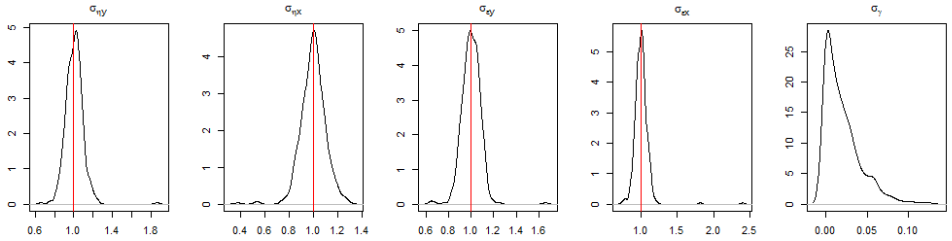

(b) $T = 500$

Figure A.4 Distribution of the indirect inference estimators of the static parameters of the nonlinear model, $\tau = \left(\sigma_{\eta,y}, \sigma_{\eta,x}, \sigma_{\varepsilon,y}, \sigma_{\varepsilon,x}, \sigma_{\gamma}\right)'$, based on the Monte Carlo replicates, when the DGP of ρ_t is a fast sine function; $S = 3$, $n_{\text{sim}} = 500$. The red lines represent the true values of the parameters.

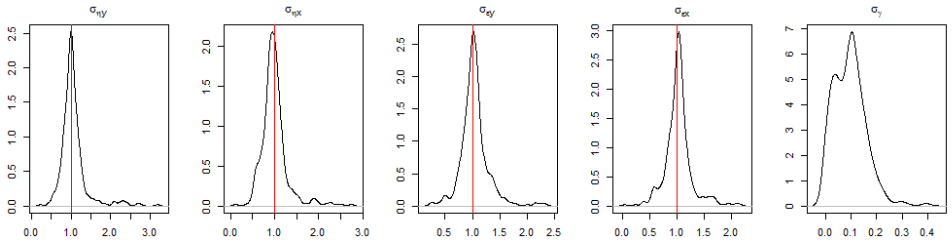

(a) $T = 200$

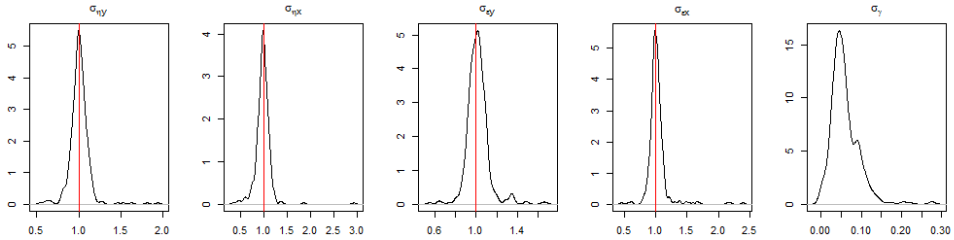

(b) $T = 500$

Figure A.5 Distribution of the indirect inference estimators of the static parameters of the nonlinear model, $\tau = \left(\sigma_{\eta,y}, \sigma_{\eta,x}, \sigma_{\varepsilon,y}, \sigma_{\varepsilon,x}, \sigma_{\gamma}\right)'$, based on the Monte Carlo replicates, when the DGP of ρ_t is a step function; $S = 3$, $n_{\text{sim}} = 500$. The red lines represent the true values of the parameters.

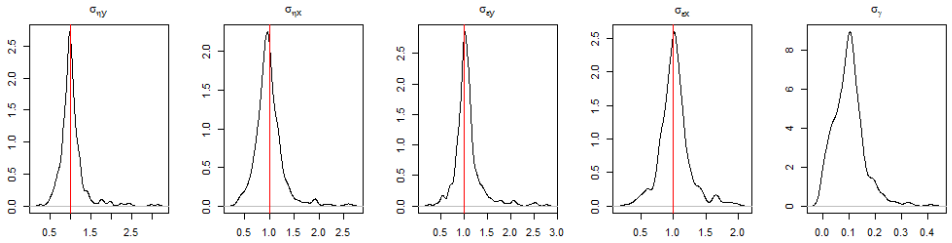

(a) $T = 200$

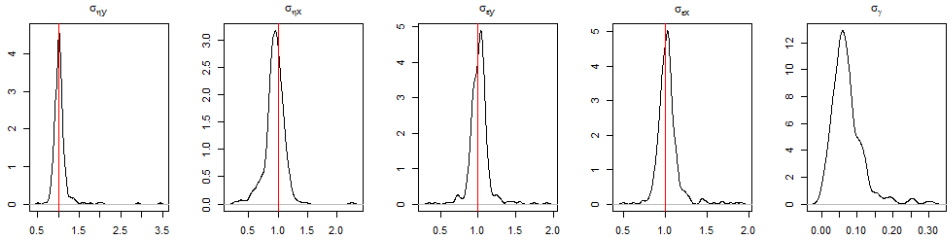

(b) $T = 500$

Figure A.6 Distribution of the indirect inference estimators of the static parameters of the nonlinear model, $\tau = \left(\sigma_{\eta,y}, \sigma_{\eta,x}, \sigma_{\varepsilon,y}, \sigma_{\varepsilon,x}, \sigma_{\gamma}\right)'$, based on the Monte Carlo replicates, when the DGP of ρ_t is a ramp function; $S = 3$, $n_{\text{sim}} = 500$. The red lines represent the true values of the parameters.

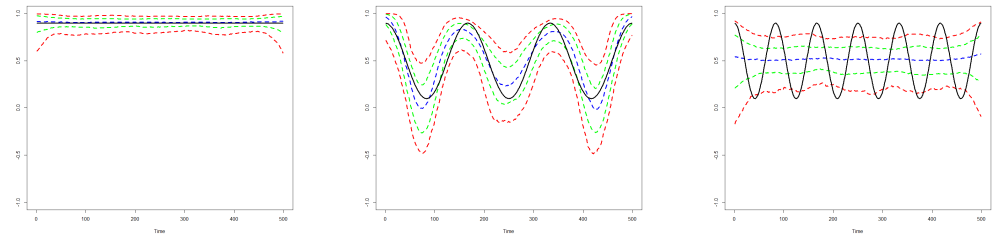

(a) Constant (b) Sine (c) Fast sine

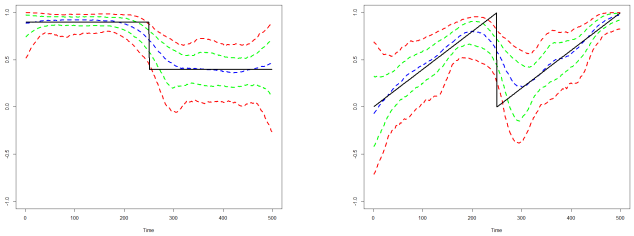

(d) Step (e) Ramp

Figure A.7 True process of ρ_t (black) together with the 95% (red), 80% (green) confidence bands, and the median (blue) of the simulation estimates for the cubic splines estimator of ρ_t. $T = 500$, $S = 3$, $M = 5000$, $n_{\text{sim}} = 500$.

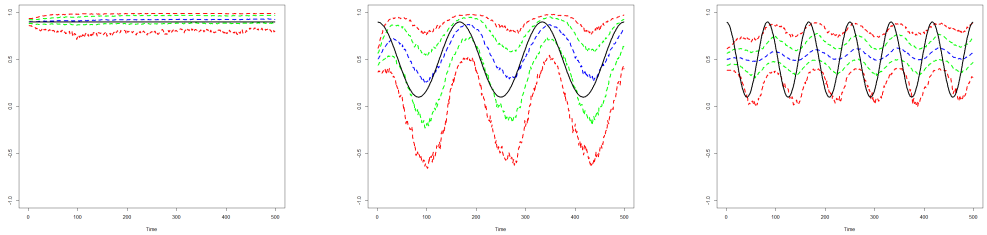

(a) Constant (b) Sine (c) Fast sine

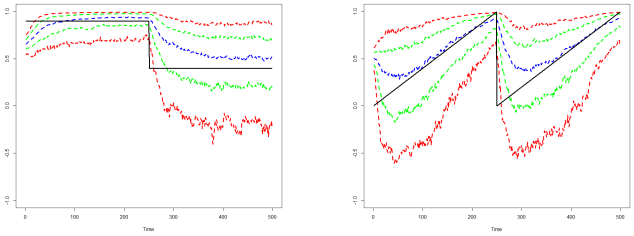

(d) Step (e) Ramp

Figure A.8 True process of ρ_t (black) together with the 95% (red), 80% (green) confidence bands, and the median (blue) of the simulation estimates for the Rao-Blackwellised bootstrap filter estimator of ρ_t. $T = 500$, $S = 3$, $M = 5000$, $n_{\text{sim}} = 500$.

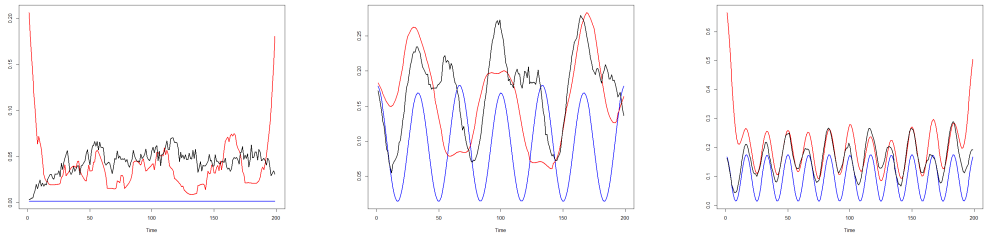

(a) Constant (b) Sine (c) Fast sine

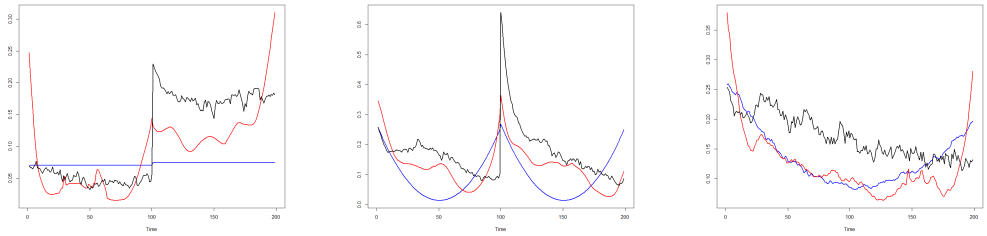

(d) Step (e) Ramp (f) Random walk

Figure A.9 MSE of the cubic splines (red), the Rao-Blackwellised bootstrap filter (black) and the constant (blue) estimators of ρ_t, over time. $T = 200$, $S = 3$, $M = 5000$, $n_{\text{sim}} = 500$.

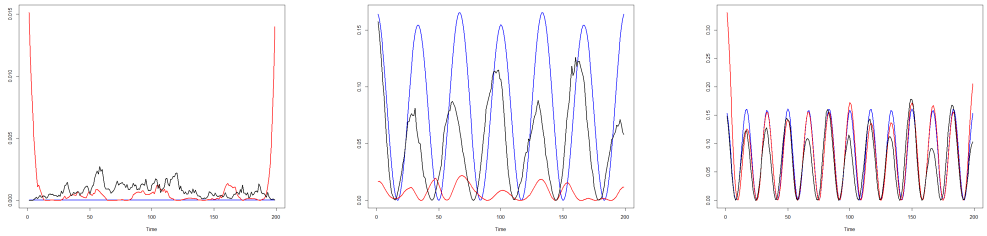

(a) Constant (b) Sine (c) Fast sine

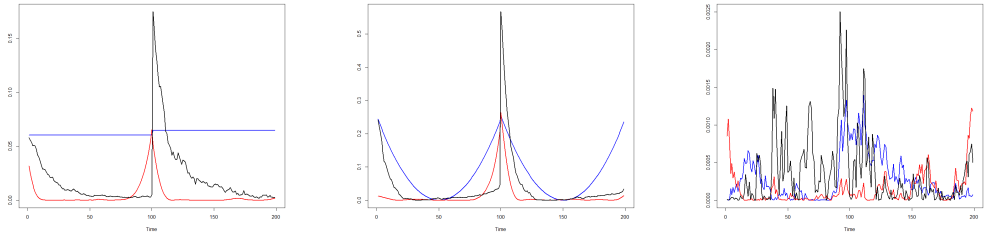

(d) Step (e) Ramp (f) Random walk

Figure A.10 Squared bias of the cubic splines (red), the Rao-Blackwellised bootstrap filter (black) and the constant (blue) estimators of ρ_t, over time. $T = 200$, $S = 3$, $M = 5000$, $n_{\text{sim}} = 500$.

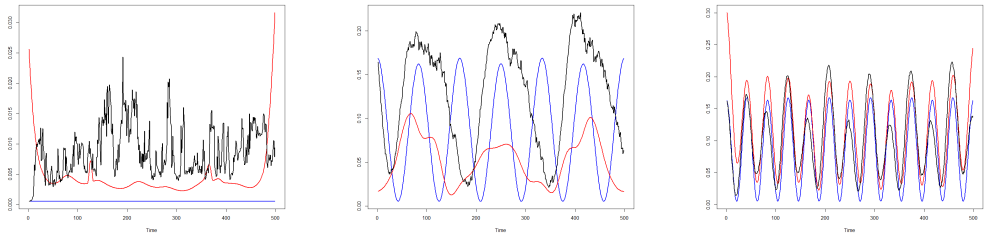

(a) Constant (b) Sine (c) Fast sine

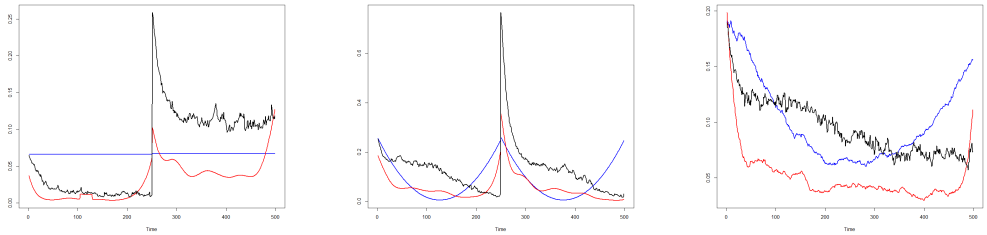

(d) Step (e) Ramp (f) Random walk

Figure A.11 MSE of the cubic splines (red), the Rao-Blackwellised bootstrap filter (black) and the constant (blue) estimators of ρ_t, over time. $T = 500$, $S = 3$, $M = 5000$, $n_{\text{sim}} = 500$.

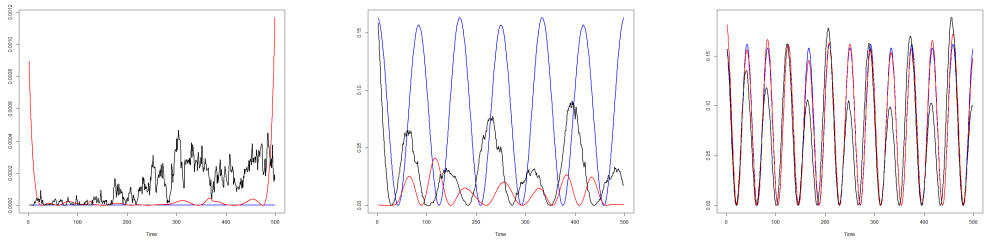

(a) Constant (b) Sine (c) Fast sine

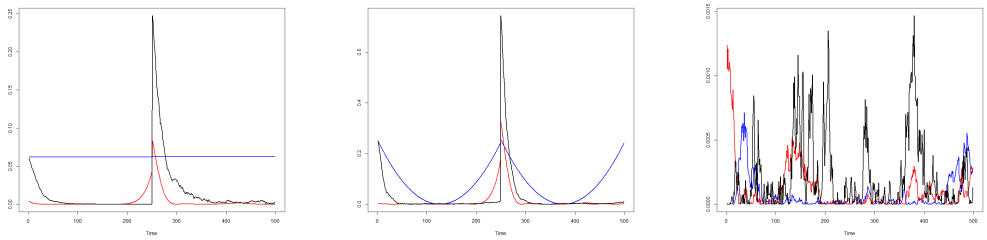

(d) Step (e) Ramp (f) Random walk

Figure A.12 Squared bias of the cubic splines (red), the Rao-Blackwellised bootstrap filter (black) and the constant (blue) estimators of ρ_t, over time. $T = 500$, $S = 3$, $M = 5000$, $n_{\text{sim}} = 500$.

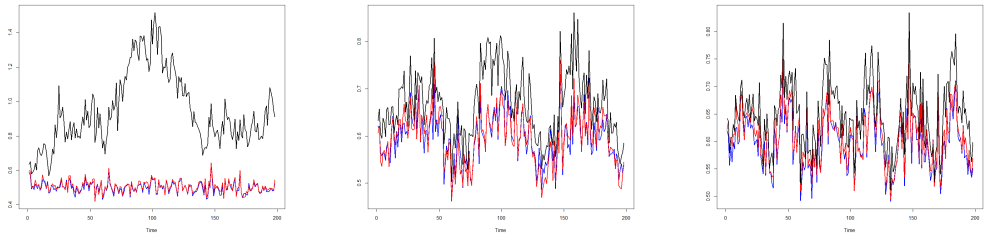

(a) Constant (b) Sine (c) Fast sine

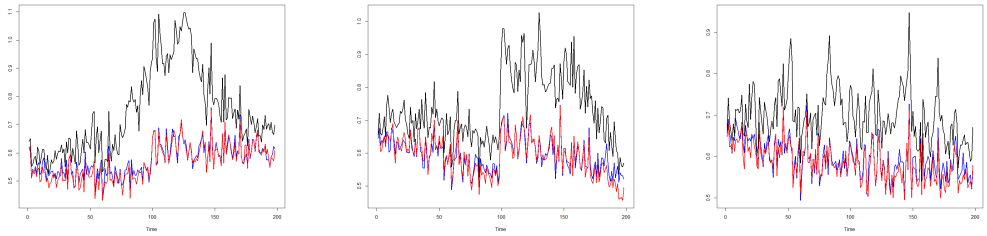

(d) Step (e) Ramp (f) Random walk

Figure A.13 MSE, over time, of the Kalman filter estimator of $L_{y,t}$ when ρ_t is estimated by the cubic splines (red) and the Rao-Blackwellised bootstrap filter (black) methods, and as time-constant (blue). $T = 200$, $S = 3$, $M = 5000$, $n_{\text{sim}} = 500$.

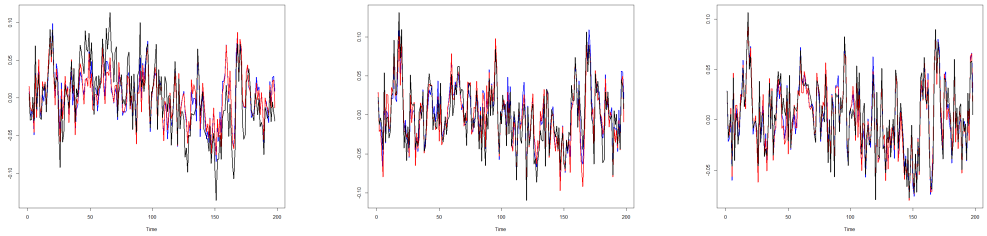

(a) Constant (b) Sine (c) Fast sine

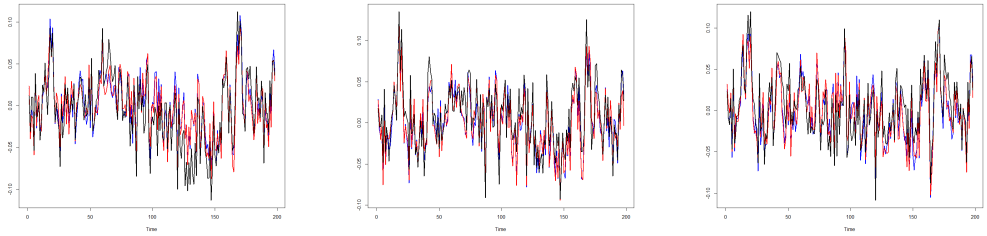

(d) Step (e) Ramp (f) Random walk

Figure A.14 Squared bias, over time, of the Kalman filter estimator of $L_{y,t}$ when ρ_t is estimated by the cubic splines (red) and the Rao-Blackwellised bootstrap filter (black) methods, and as time-constant (blue). $T = 200$, $S = 3$, $M = 5000$, $n_{\text{sim}} = 500$.

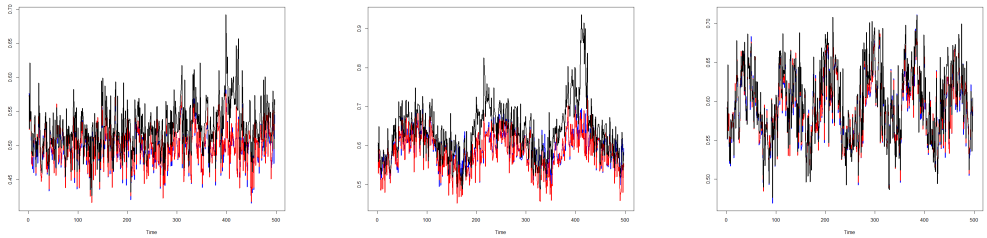

(a) Constant (b) Sine (c) Fast sine

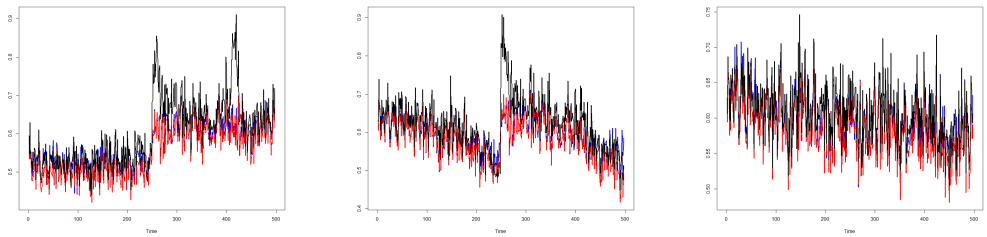

(d) Step (e) Ramp (f) Random walk

Figure A.15 MSE, over time, of the Kalman filter estimator of $L_{y,t}$ when ρ_t is estimated by the cubic splines (red) and the Rao-Blackwellised bootstrap filter (black) methods, and as time-constant (blue). $T = 500$, $S = 3$, $M = 5000$, $n_{\text{sim}} = 500$.

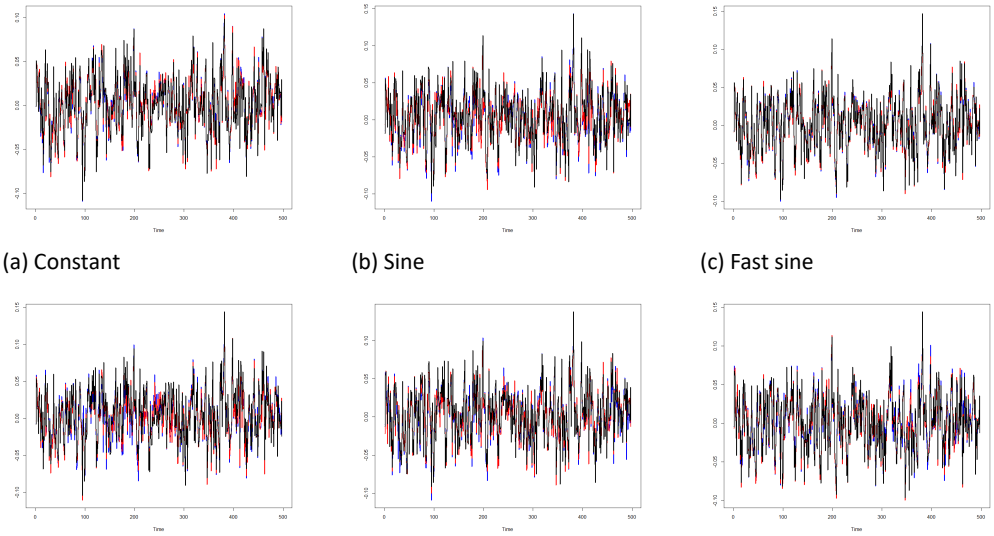

(a) Constant (b) Sine (c) Fast sine

(d) Step (e) Ramp (f) Random walk

Figure A.16 Squared bias, over time, of the Kalman filter estimator of $L_{y,t}$ when ρ_t is estimated by the cubic splines (red) and the Rao-Blackwellised bootstrap filter (black) methods, and as time-constant (blue). $T = 500$, $S = 3$, $M = 5000$, $n_{\text{sim}} = 500$.

B Additional results from the empirical application

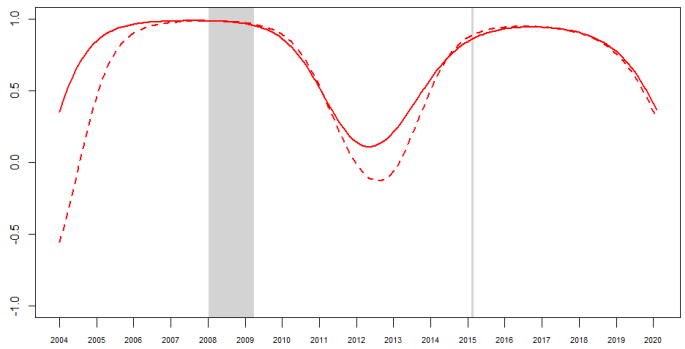

(a) Cubic splines

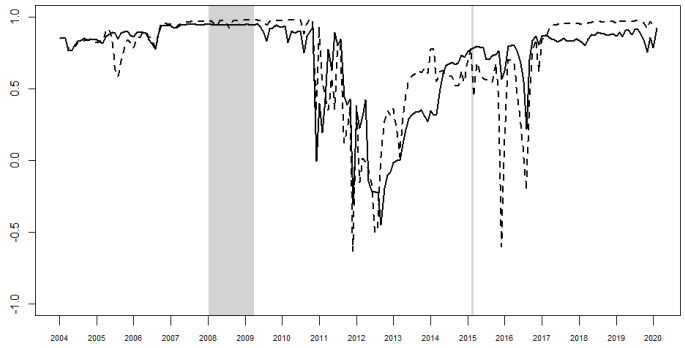

(b) RBBF

Figure B.1 Cubic splines and RBBF estimates of ρ_t, from the Dutch labour force model extended with the auxiliary series of claimant counts (described in Section 2). Monthly data from January 2004 until March 2020 ($T = 195$), $S = 5$, $M = 5000$. The dashed lines refer to the setting where the knots for the cubic splines approach are approximately equally distant by fixing February 2015 as one of them, otherwise they correspond to the quartiles of the sample. The first shaded area represent the recession period due to the financial crisis of 2018, whereas the second one refers to the legislative change of February 2015.

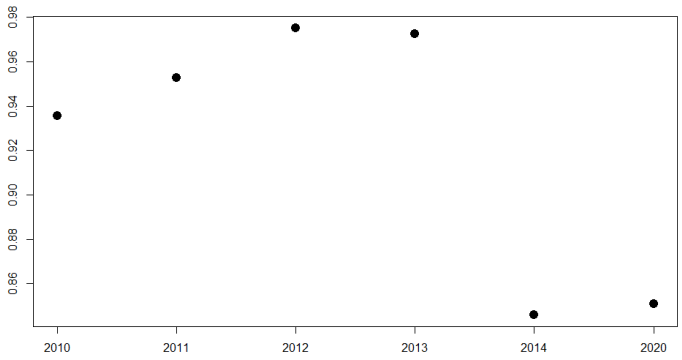

Figure B.2 Estimates of the correlation parameter when this is treated as time-constant, obtained with monthly data observed from January 2004 up to and including the year displayed on the horizontal axis. The results refer to the Dutch labour force model extended with the auxiliary series of claimant counts (described in Section 2).

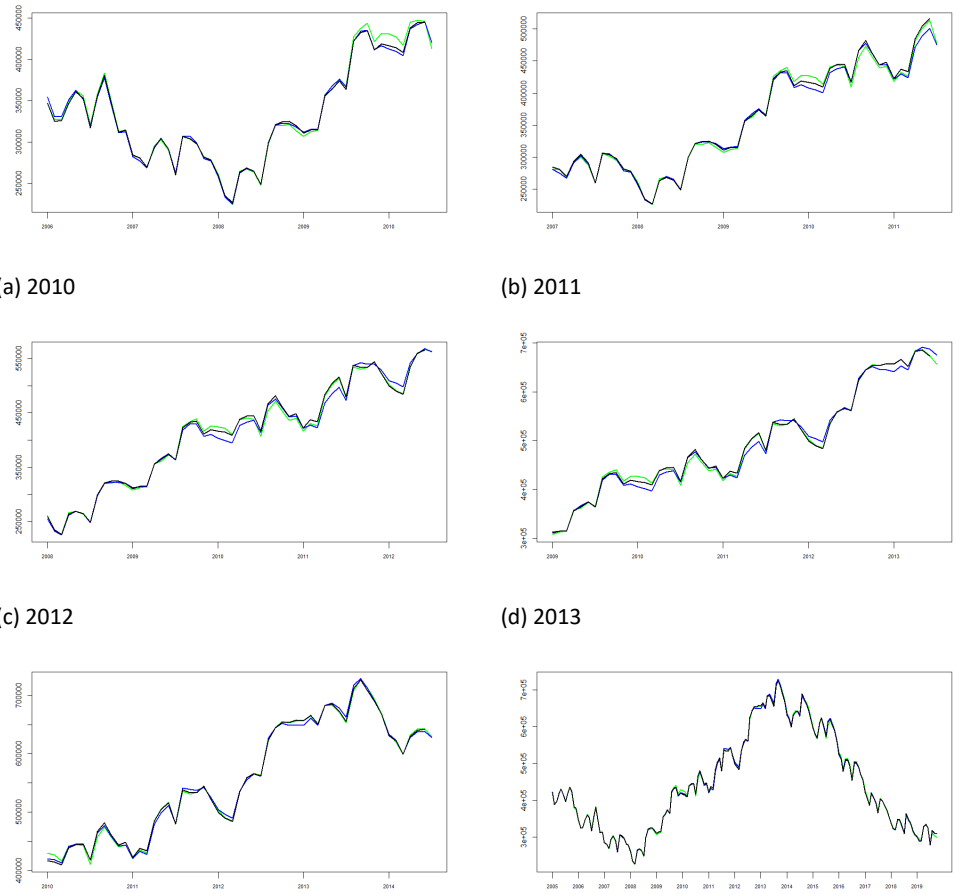

(a) 2010 (b) 2011

(c) 2012 (d) 2013

(e) 2014 (f) 2020

Figure B.3 Kalman filter estimates of $\theta_{y,t}$ in the Dutch labour force model (described in Section 2). The green lines refer to the model without auxiliary series. The blue and black lines refer to the model extended with the auxiliary series of claimant counts, when the correlation is estimated as time constant and with the RBBF, respectively. Each panel shows the results obtained with monthly data observed from January 2004 up to and including the year displayed in the respective caption. We do not always show estimates for all time periods in order to facilitate the comparison among panels.

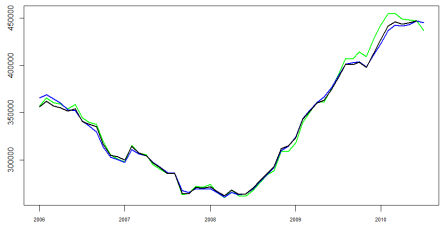

(a) 2010

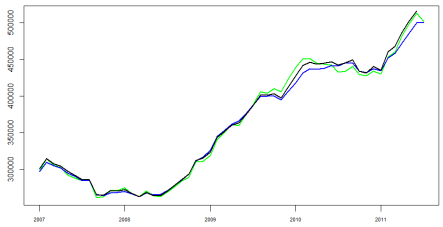

(b) 2011

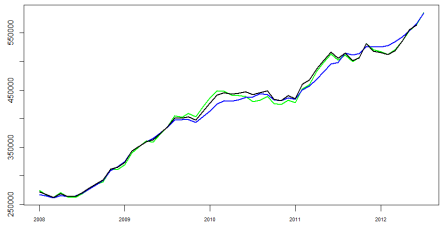

(c) 2012

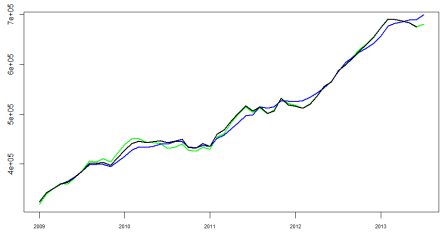

(d) 2013

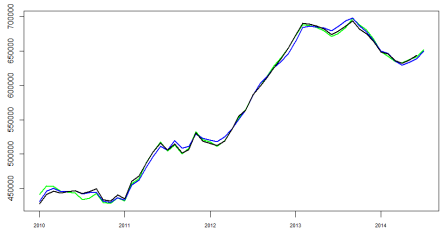

(e) 2014

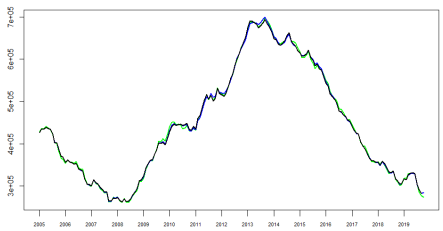

(f) 2020

Figure B.4 Kalman filter estimates of $L_{y,t}$ in the Dutch labour force model (described in Section 2). The green lines refer to the model without auxiliary series. The blue and black lines refer to the model extended with the auxiliary series of claimant counts, when the correlation is estimated as time constant and with the RBBF, respectively. Each panel shows the results obtained with monthly data observed from January 2004 up to and including the year displayed in the respective caption. We do not always show estimates for all time periods in order to facilitate the comparison among panels.

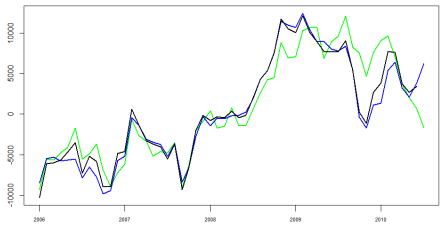

(a) 2010

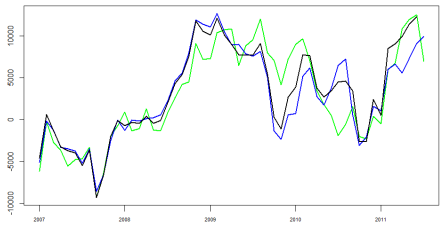

(b) 2011

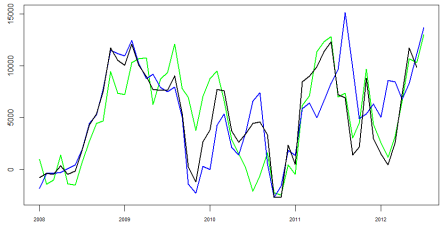

(c) 2012

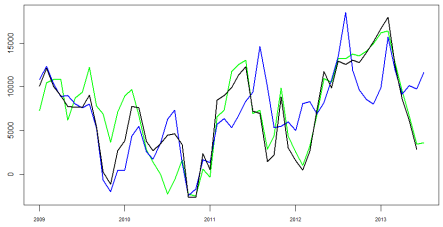

(d) 2013

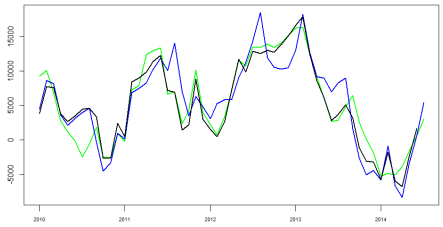

(e) 2014

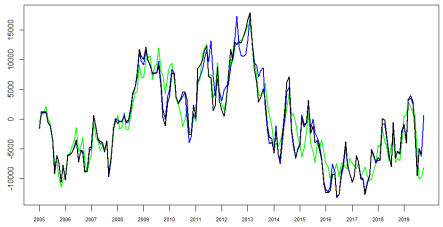

(f) 2020

Figure B.5 Kalman filter estimates of $R_{y,t}$ in the Dutch labour force model (described in Section 2). The green lines refer to the model without auxiliary series. The blue and black lines refer to the model extended with the auxiliary series of claimant counts, when the correlation is estimated as time constant and with the RBBF, respectively. Each panel shows the results obtained with monthly data observed from January 2004 up to and including the year displayed in the respective caption. We do not always show estimates for all time periods in order to facilitate the comparison among panels.

(a) 2010 (b) 2011

(c) 2012 (d) 2013

(e) 2014 (f) 2020

Figure B.6 Estimated variances, var̂ $\left(\hat{\theta}_{y,t}\right)$, of the Kalman filter estimates of $\theta_{y,t}$ in the Dutch labour force model (described in Section 2). The green lines refer to the model without auxiliary series. The blue and black lines refer to the model extended with the auxiliary series of claimant counts, when the correlation is estimated as time constant and with the RBBF, respectively. Each panel shows the results obtained with monthly data observed from January 2004 up to and including the year displayed in the respective caption. We do not always show estimates for all time periods in order to facilitate the comparison among panels.

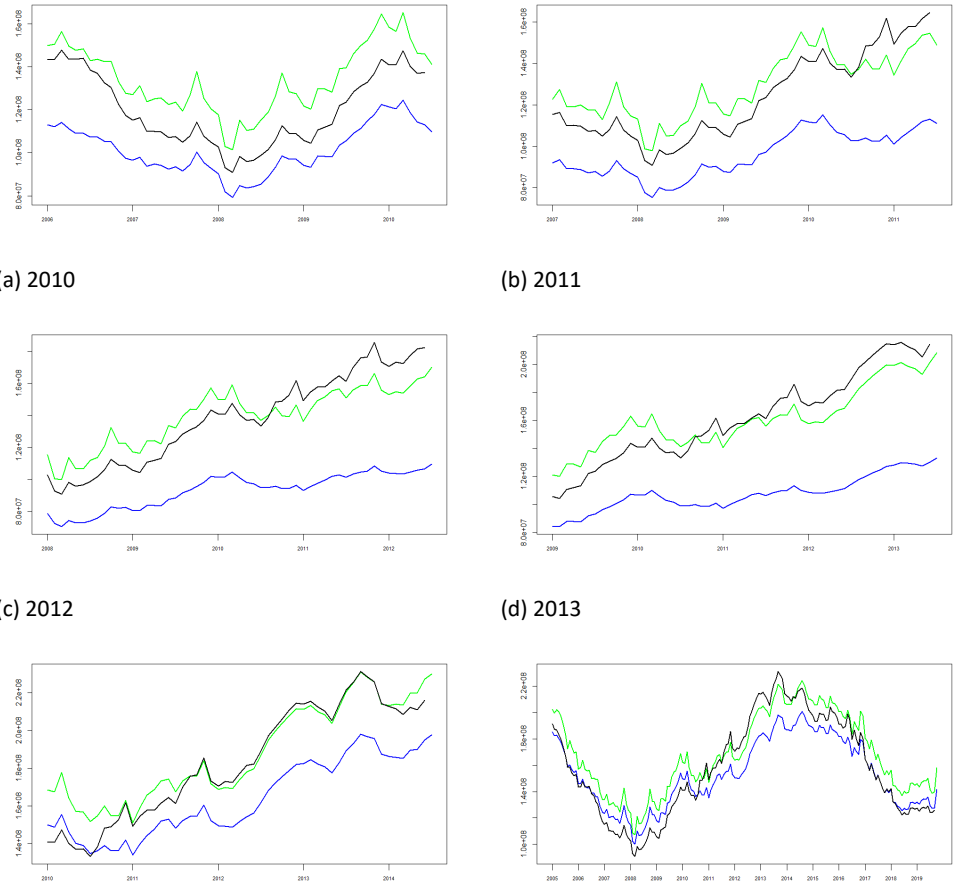

(a) 2010 (b) 2011

(c) 2012 (d) 2013

(e) 2014 (f) 2020

Figure B.7 Estimated variances, var̂ $\left(\hat{L}_{y,t}\right)$, of the Kalman filter estimates of $L_{y,t}$ in the Dutch labour force model (described in Section 2). The green lines refer to the model without auxiliary series. The blue and black lines refer to the model extended with the auxiliary series of claimant counts, when the correlation is estimated as time constant and with the RBBF, respectively. Each panel shows the results obtained with monthly data observed from January 2004 up to and including the year displayed in the respective caption. We do not always show estimates for all time periods in order to facilitate the comparison among panels.

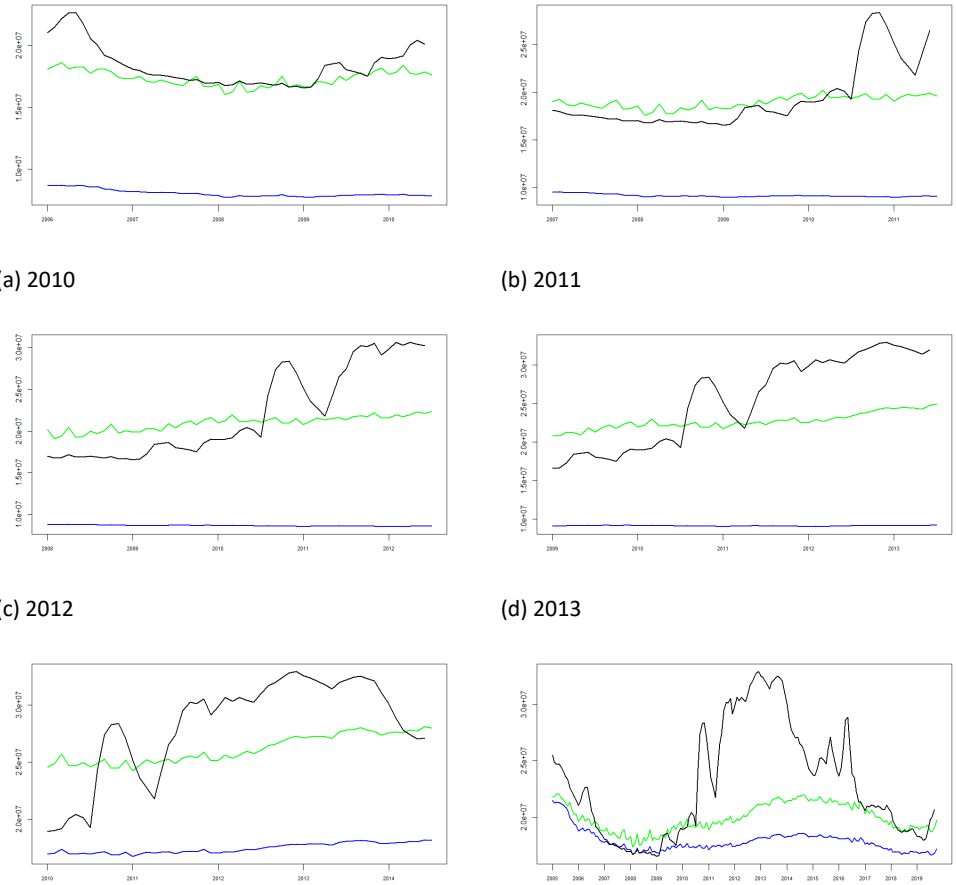

(a) 2010 (b) 2011

(c) 2012 (d) 2013

(e) 2014 (f) 2020

Figure B.8 Estimated variances, var̂ $\left(\hat{R}_{y,t}\right)$, of the Kalman filter estimates of $R_{y,t}$ in the Dutch labour force model (described in Section 2). The green lines refer to the model without auxiliary series. The blue and black lines refer to the model extended with the auxiliary series of claimant counts, when the correlation is estimated as time constant and with the RBBF, respectively. Each panel shows the results obtained with monthly data observed from January 2004 up to and including the year displayed in the respective caption. We do not always show estimates for all time periods in order to facilitate the comparison among panels.

Colophon

Publisher
Statistics Netherlands
Henri Faasdreef 312, 2492 JP The Hague
www.cbs.nl

Prepress
Statistics Netherlands, Grafimedia

Design
Edenspiekermann

Information
Telephone +31 88 570 70 70, fax +31 70 337 59 94
Via contact form: www.cbs.nl/information